



U.S. Department of  
Transportation

Federal Railroad  
Administration

# Inspection of Concrete Ties Using Sonic/Ultrasonic Impact Velocity and Impact Echo Measurements

Office of Research,  
Development  
and Technology  
Washington, DC 20590



#### NOTICE

This document is disseminated under the sponsorship of the Department of Transportation in the interest of information exchange. The United States Government assumes no liability for its contents or use thereof. Any opinions, findings and conclusions, or recommendations expressed in this material do not necessarily reflect the views or policies of the United States Government, nor does mention of trade names, commercial products, or organizations imply endorsement by the United States Government. The United States Government assumes no liability for the content or use of the material contained in this document.

#### NOTICE

The United States Government does not endorse products or manufacturers. Trade or manufacturers' names appear herein solely because they are considered essential to the objective of this report.

# REPORT DOCUMENTATION PAGE

*Form Approved*  
**OMB No. 0704-0188**

Public reporting burden for this collection of information is estimated to average 1 hour per response, including the time for reviewing instructions, searching existing data sources, gathering and maintaining the data needed, and completing and reviewing the collection of information. Send comments regarding this burden estimate or any other aspect of this collection of information, including suggestions for reducing this burden, to Washington Headquarters Services, Directorate for Information Operations and Reports, 1215 Jefferson Davis Highway, Suite 1204, Arlington, VA 22202-4302, and to the Office of Management and Budget, Paperwork Reduction Project (0704-0188), Washington, DC 20503.

1. AGENCY USE ONLY (Leave blank)	2. REPORT DATE September 2018	3. REPORT TYPE AND DATES COVERED Technical Report July 2012–December 2013
----------------------------------	----------------------------------	--

4. TITLE AND SUBTITLE Inspection of Concrete Ties Using Sonic/Ultrasonic Impact Velocity and Impact Echo Measurements	5. FUNDING NUMBERS DTFR53-12-C-00022 DTFR53-14-C-00027
--	--

6. AUTHOR(S) Paul S. Fisk	
------------------------------	--

7. PERFORMING ORGANIZATION NAME(S) AND ADDRESS(ES) NDT Corporation 153 Clinton Road Sterling, MA 01564	8. PERFORMING ORGANIZATION REPORT NUMBER FD-2
---	--

9. SPONSORING/MONITORING AGENCY NAME(S) AND ADDRESS(ES) U.S. Department of Transportation Federal Railroad Administration Office of Railroad Policy and Development Office of Research, Development and Technology Washington, DC 20590	10. SPONSORING/MONITORING AGENCY REPORT NUMBER  DOT/FRA/ORD-18/32
--	---

11. SUPPLEMENTARY NOTES COR: Hugh Thompson (Phase1), Cameron Stuart (Phase 2)
--

12a. DISTRIBUTION/AVAILABILITY STATEMENT This document is available to the public through the FRA Web site at <a href="http://www.fra.dot.gov">http://www.fra.dot.gov</a> .	12b. DISTRIBUTION CODE
--	------------------------

13. ABSTRACT (Maximum 200 words) This report documents NDT Corporation’s development of a non-destructive system for inspecting the internal condition of concrete crossties using sonic/ultrasonic impact velocity (IV) and impact echo (IE) measurements. The system, developed at NDT’s facility and tested on numerous railroads in the U.S., is a significant improvement over traditional visual inspection techniques because it objectively quantifies the internal tie condition. The work was completed in two phases. Phase 1 was the initial development and proof of concept testing period, and Phase 2 developed an automated prototype and completed field validation tests. Destructive testing of concrete ties reveals that this new system can accurately differentiate between undamaged and damaged ties with sufficient resolution to grade ties into five classes. This grading scheme was created to closely match similar grading schemes used by Union Pacific Railroad (UP), Amtrak, and other railroads. An on-rail carriage was equipped with a solenoid impactor energy source, microphone sensors, and a data processing and display computer. Software was developed for data acquisition and real-time data analysis. The system included a real-time paint marking of deteriorated ties. Field tests in both yard and revenue service track locations have demonstrated the accuracy and repeatability of the system.
---

14. SUBJECT TERMS Concrete, crossties, ties, Rayleigh waves, impact echo, impact velocity	15. NUMBER OF PAGES 103
--	----------------------------

	16. PRICE CODE
--	----------------

17. SECURITY CLASSIFICATION OF REPORT Unclassified	18. SECURITY CLASSIFICATION OF THIS PAGE Unclassified	19. SECURITY CLASSIFICATION OF ABSTRACT Unclassified	20. LIMITATION OF ABSTRACT
---	--	---	----------------------------

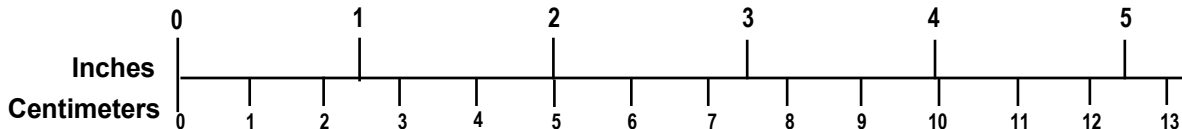
# METRIC/ENGLISH CONVERSION FACTORS

## ENGLISH TO METRIC

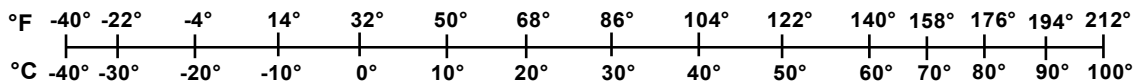
## METRIC TO ENGLISH

<p><b>LENGTH (APPROXIMATE)</b></p> <p>1 inch (in) = 2.5 centimeters (cm)</p> <p>1 foot (ft) = 30 centimeters (cm)</p> <p>1 yard (yd) = 0.9 meter (m)</p> <p>1 mile (mi) = 1.6 kilometers (km)</p>	<p><b>LENGTH (APPROXIMATE)</b></p> <p>1 millimeter (mm) = 0.04 inch (in)</p> <p>1 centimeter (cm) = 0.4 inch (in)</p> <p>1 meter (m) = 3.3 feet (ft)</p> <p>1 meter (m) = 1.1 yards (yd)</p> <p>1 kilometer (km) = 0.6 mile (mi)</p>
<p><b>AREA (APPROXIMATE)</b></p> <p>1 square inch (sq in, in<sup>2</sup>) = 6.5 square centimeters (cm<sup>2</sup>)</p> <p>1 square foot (sq ft, ft<sup>2</sup>) = 0.09 square meter (m<sup>2</sup>)</p> <p>1 square yard (sq yd, yd<sup>2</sup>) = 0.8 square meter (m<sup>2</sup>)</p> <p>1 square mile (sq mi, mi<sup>2</sup>) = 2.6 square kilometers (km<sup>2</sup>)</p> <p>1 acre = 0.4 hectare (he) = 4,000 square meters (m<sup>2</sup>)</p>	<p><b>AREA (APPROXIMATE)</b></p> <p>1 square centimeter (cm<sup>2</sup>) = 0.16 square inch (sq in, in<sup>2</sup>)</p> <p>1 square meter (m<sup>2</sup>) = 1.2 square yards (sq yd, yd<sup>2</sup>)</p> <p>1 square kilometer (km<sup>2</sup>) = 0.4 square mile (sq mi, mi<sup>2</sup>)</p> <p>10,000 square meters (m<sup>2</sup>) = 1 hectare (ha) = 2.5 acres</p>
<p><b>MASS - WEIGHT (APPROXIMATE)</b></p> <p>1 ounce (oz) = 28 grams (gm)</p> <p>1 pound (lb) = 0.45 kilogram (kg)</p> <p>1 short ton = 2,000 pounds (lb) = 0.9 tonne (t)</p>	<p><b>MASS - WEIGHT (APPROXIMATE)</b></p> <p>1 gram (gm) = 0.036 ounce (oz)</p> <p>1 kilogram (kg) = 2.2 pounds (lb)</p> <p>1 tonne (t) = 1,000 kilograms (kg) = 1.1 short tons</p>
<p><b>VOLUME (APPROXIMATE)</b></p> <p>1 teaspoon (tsp) = 5 milliliters (ml)</p> <p>1 tablespoon (tbsp) = 15 milliliters (ml)</p> <p>1 fluid ounce (fl oz) = 30 milliliters (ml)</p> <p>1 cup (c) = 0.24 liter (l)</p> <p>1 pint (pt) = 0.47 liter (l)</p> <p>1 quart (qt) = 0.96 liter (l)</p> <p>1 gallon (gal) = 3.8 liters (l)</p> <p>1 cubic foot (cu ft, ft<sup>3</sup>) = 0.03 cubic meter (m<sup>3</sup>)</p> <p>1 cubic yard (cu yd, yd<sup>3</sup>) = 0.76 cubic meter (m<sup>3</sup>)</p>	<p><b>VOLUME (APPROXIMATE)</b></p> <p>1 milliliter (ml) = 0.03 fluid ounce (fl oz)</p> <p>1 liter (l) = 2.1 pints (pt)</p> <p>1 liter (l) = 1.06 quarts (qt)</p> <p>1 liter (l) = 0.26 gallon (gal)</p> <p>1 cubic meter (m<sup>3</sup>) = 36 cubic feet (cu ft, ft<sup>3</sup>)</p> <p>1 cubic meter (m<sup>3</sup>) = 1.3 cubic yards (cu yd, yd<sup>3</sup>)</p>
<p><b>TEMPERATURE (EXACT)</b></p> <p><math>[(x-32)(5/9)] \text{ } ^\circ\text{F} = y \text{ } ^\circ\text{C}</math></p>	<p><b>TEMPERATURE (EXACT)</b></p> <p><math>[(9/5) y + 32] \text{ } ^\circ\text{C} = x \text{ } ^\circ\text{F}</math></p>

## QUICK INCH - CENTIMETER LENGTH CONVERSION



## QUICK FAHRENHEIT - CELSIUS TEMPERATURE CONVERSION



For more exact and or other conversion factors, see NIST Miscellaneous Publication 286, Units of Weights and Measures. Price \$2.50 SD Catalog No. C13 10286

Updated 6/17/98



## **Acknowledgements**

---

NDT acknowledges the hard work of our project team: Benson Armitage, technical supervisor; Mr. Eric de Rivera, Mechanical Engineer; and Mr. Robert Sheehan, Software Engineer. Without their hard work and attention to details, this project could not have been completed. We would like to acknowledge Mr. Chris Windangle of Red Transfer Logistics for providing access to a short stretch of rail with concrete ties less than 1 hour from NDT's location. This was invaluable as it provided NDT with the opportunity to test without large logistical effort.

# Contents

---

Executive Summary .....	1
1. Introduction .....	2
1.1 Background .....	2
1.2 IV and IE Waves in Concrete .....	2
1.3 Objectives .....	3
1.4 Overall Approach .....	4
1.5 Scope .....	4
1.6 Organization of Report .....	4
2. Phase 1 – Prototype System Development and Testing .....	5
2.1 Prototype Measurement Technique .....	5
2.2 Union Pacific Railroad Prototype System Testing .....	6
2.3 Metro-North Railroad System Automation and Testing .....	11
2.4 UP Automated Testing .....	13
2.5 UP Repeatability Testing .....	15
2.6 Phase 1 – Conclusions .....	16
3. Phase 2 – Production Prototype Development and Demonstration .....	17
3.1 Scope .....	17
3.2 Microphone Sensors .....	17
3.3 Alternate Energy and Wave Generation System .....	22
3.4 Improved Tie Locator .....	23
3.5 Software Development .....	24
3.6 ACTT-2 System and Testing .....	25
3.7 System Testing and Demonstration .....	26
4. Conclusion .....	30
5. References .....	31
Appendix A: Union Pacific Test Results – October 2012 .....	39
Appendix B: Metro-North Test Results, March 2013 .....	93
Appendix C: Union Pacific Test Results, May 2013 .....	100
Appendix D: Repeatability Testing Data – October 2013 .....	126
Abbreviations and Acronyms .....	128

## Illustrations

---

Figure 1. Illustration of Wave Motion .....	3
Figure 2. Photo of Impact Energy Source and Sensor Array.....	5
Figure 3. IV and IE Measurements on Ties .....	6
Figure 4. Tie 2, South, Showing Horizontal Crack.....	7
Figure 5. UP Tie Inspection Data and Grading.....	9
Figure 6. Example of Internal Cracking .....	10
Figure 7. Tie Rating Decision Tree.....	11
Figure 8. ACTT-1 System on Metro-North Railroad .....	12
Figure 9. ACTT-1 System on UP Track .....	13
Figure 10. Handheld (Array) Versus Automatic Ranking.....	14
Figure 11. UP Ties with Center Cracking.....	15
Figure 12. Comparison of IV Data Recorded with Contact and Microphone Sensors.....	17
Figure 13. Microphone Sensor.....	18
Figure 14. Shotgun Microphone Mount.....	19
Figure 15. Shotgun Microphone Versus Contact Sensors .....	20
Figure 16. Microphone System Repeatability Test Results.....	21
Figure 17. Ball End Impactors .....	22
Figure 18. Ball End “Tapper” Installed on ACTT-2.....	23
Figure 19. Magnetic Proximity Switch Installed on ACTT-2 .....	24
Figure 20. Rayleigh Wave Velocity Decision Tree for Rating Ties.....	25
Figure 21. ACTT-2 System On-Rail and Folded for Transport.....	26
Figure 22. ACTT-2 Test Results.....	27
Figure 23. ACTT-2 Demonstration at the TTC .....	28
Figure 24. ACTT-2 Demonstration at the 2016 International Crosstie and Fastener Symposium, Urbana, IL.....	29

## Executive Summary

---

This report documents the work performed by NDT Corporation (NDT), with funding by the Federal Railroad Administration (FRA), to develop a non-destructive system for inspecting the internal condition of concrete crossties using sonic/ultrasonic impact velocity (IV) and impact echo (IE) measurements. The system is a significant improvement over traditional, visual inspection techniques because it objectively quantifies the internal tie condition. The work was completed in two phases. Phase 1 was executed between July 2012 and December 2013 and accomplished the initial development of the system, as well as proof of concept testing. During Phase 2, executed between October 2014 and June 2016, NDT developed an automated prototype and completed field validation tests. NDT completed all development at its facilities in Massachusetts and performed numerous field trials on railroads throughout the United States.

Destructive testing of concrete ties revealed that this new system can accurately differentiate between undamaged and damaged ties with sufficient resolution to grade ties into five classes. This grading scheme has been shown to closely match similar grading schemes used by railroads. NDT developed an on-rail carriage with a solenoid impactor energy source, microphone sensors, and a data processing and display computer.

NDT wrote custom software for data acquisition and real-time data analysis. The software rates each crosstie on a 1 to 5 scale (1 = no damage and 5 = severely damaged) based on the wave velocity through the crosstie. The rating system corresponds well to systems used by Amtrak and Union Pacific Railroad. Paint marking is automatically applied to a crosstie with a rank of 4 or 5. Field testing results showed that the Automated Concrete Tie Tester (ACTT) system output correlated favorably with visual inspections of crossties. The system included a real-time paint system to mark deteriorated ties. Field tests in both yard and revenue service track locations have demonstrated the accuracy and repeatability of the system.

NDT designed and constructed a light-weight rail carriage, ACTT-2, to support and move the system along the track. The carriage weighed approximately 150 pounds. This system can also be modified to be pushed, towed or suspended by a high-rail vehicle. The next step is to increase the rate that the ACTT system can acquire, archive, interpret and mark distressed ties from 3 mph to 10 to 20 mph.

# 1. Introduction

---

This section of the report discusses the need for a non-destructive in-track evaluation of concrete ties, as well as presenting the objectives of this research project conducted by the NDT Corporation, and provides the technical description of the measurement technique.

## 1.1 Background

Current concrete crosstie inspection techniques are based on visual inspections of the exposed top surface and limited areas of the side and ends of crossties. Most of the crosstie is hidden from view by ballast and serious defects may not be visible. It is also difficult to quantify the severity of flaws based solely on a visual inspection. Comparing visual results from previous inspections is subjective as crosstie deterioration can be rapid. In areas where a deteriorated, cracked crosstie is found, there may be numerous consecutive fractured weakened crossties found in subsequent inspections. This poses a safety risk and makes maintenance planning difficult.

Concrete crossties are an essential component of the U.S. rail system. A reliable, scientific assessment of the structural performance of each crosstie is essential to ensure safe rail operations. Data indicating specific locations of weakening concrete crossties, along with deterioration rates, can provide useful information to maintenance planners. Repair planning might include identifying weak crossties for replacement before adjacent crossties deteriorate, thus prolonging the useful life of the crossties and extending the time between scheduled crosstie replacements or determine when a stretch of crossties should be scheduled for replacement.

Impact velocity (IV) and impact echo (IE) measurements have been used for decades to evaluate concrete. IV measurements (American Society for Testing and Materials [ASTM] C-597) record the time required for compressional and shear waves to propagate a given distance through concrete [1]. These velocity values with an approximate concrete density can be used to determine the moduli (elastic strength properties) and strength values of the concrete. IE measurements (ASTM C-1383) record the frequency that concrete resonates at as a result of compressional waves being reflected back and forth between two surfaces [2]. Seismic body and surface waves (compressional, shear and Rayleigh) that propagate through pre-stressed concrete rail road ties can be used to make an assessment of the condition and integrity of each tie. Adapting impact velocity testing to concrete crossties will improve the accuracy, repeatability, and thoroughness of crosstie inspection activities.

## 1.2 IV and IE Waves in Concrete

IV and IE sonic/ultrasonic measurement waves are made by generating a relatively low energy, discrete, wide band impulse with a projectile impact and measuring the time required for the waves to travel from the impact spot to a receiving sensor. The transmitted energy is in the form of three principal wave types: compressional (contraction/expansion, spring-like particle motion), shear (traction-sliding motion), and surface waves (combination of motions), as illustrated in Figure 1.

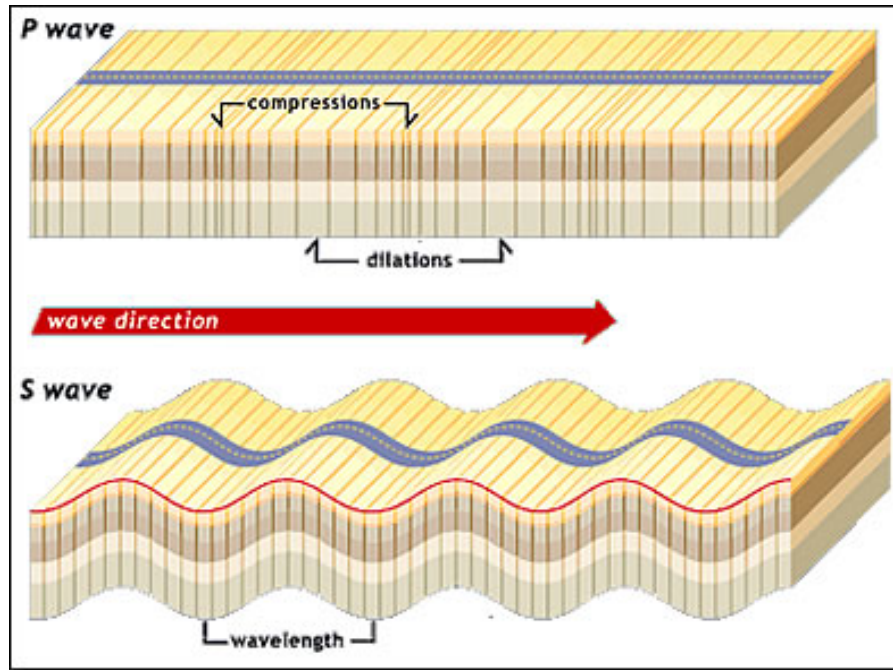


**Figure 1. Illustration of Wave Motion**

(Source: <http://www.sms-tsunami-warning.com/pages/seismic-waves#.WxF6LO4vxph>)

The velocity at which these waves propagate through the concrete is controlled by the concrete's elastic properties and internal condition. Typically, unconfined 4,000 to 5,000 psi concrete will have compressional wave velocities in the range of 12,500 to 13,500 ft./sec and shear wave velocity values in the range of 6,000 to 6,500 ft./sec. In contrast, air has a compressional wave velocity of 800 ft./sec and air does not support shear waves. Compressional and shear wave velocities are lower in fractured concrete because the signals must propagate through or around the air space contained within cracks. Greater density or severity of cracks can result in lower compressional and shear wave velocity values.

### 1.3 Objectives

The objectives of Phase 1 of this research effort were to:

1. Demonstrate that sonic/ultrasonic IV/pulse velocity (PV) and IE data can accurately access internal cracking and weakening of concrete crossties when measurements are made on the top surface of crossties.
2. Demonstrate that IV and IE data can be acquired in an automated, production manner.
3. Provide a rating of the severity of the internal (not visible) flaws in concrete crossties. This rating system should be consistent with rating systems currently used by railroads.

Phase 2 continued the research effort to improve the efficiency of concrete tie testing and improve the inspection technology to a production prototype level through automation. Specific objectives of this phase included:

1. Evaluating the use of non-contact microphone sensors and other energy sources

2. Improving the manual prototype system to use tie clips to locate sensors and the energy source near the middle of the tie
3. Developing data acquisition software that can instantaneously evaluate, rate/rank and mark ties
4. Acquiring on-rail data to evaluate production rates and develop a data base of comparison between tie conditions and IV and IE data

#### **1.4 Overall Approach**

Both phases of this research relied on a combination of laboratory development and field verification to achieve the project objectives. NDT succeeded in this development by employing an iterative process, with significant support from participating railroads. Initial development and testing of a manual, beam-type, device confirmed that the IV and IE measurements provided significant insight into the internal condition of concrete ties. Further development and testing in Phase 2, resulted in an automated, walking-speed system suitable for long distance tie evaluation. The project concluded with system demonstrations at the Transportation Technology Center (TTC) in Pueblo, CO, and at the 2016 International Crosstie and Fastener Symposium in Urbana, IL.

#### **1.5 Scope**

The scope of this report includes all development and testing activities associated with the manual system (Phase 1), and the automated system (Phase 2). Example test data is included in the body of the report and in more detail in the appendices.

#### **1.6 Organization of Report**

The report is organized chronologically based on the execution of both project phases. Section 2 contains all activities and conclusions from Phase 1, and Section 3 contains all activities and conclusions from Phase 2. The final section summarizes the state of system development and performance after completion of the project work, and gives additional insight into possible feature and configuration improvements to guide future development efforts.



## 2. Phase 1 – Prototype System Development and Testing

---

This section of the report describes the development and testing of the manual measurement system.

### 2.1 Prototype Measurement Technique

The handheld, prototype measurement beam is shown in Figure 2. To inspect a crosstie, the wave velocity is measured as the time of wave travel from the energy impact location to a linear array of sensors on the surface of the tie. Sensors are located on either side of the rail seat and energy impacts are independently generated at both ends of the tie. Data acquired by sensors 1 and 2, closest to the impact source, measures the condition of the tie from the energy impact location to the inside of the rail seat. Velocity data acquired at sensor 3 and 4, at the opposite end of the beam from the impact point, are used to evaluate for center vertical fractures. Tests are made at each end of the tie by flipping the measurement beam.



**Figure 2. Photo of Impact Energy Source and Sensor Array**

The impact source is a small, air-fired projectile and the sensors are piezo-ceramic contact type. The inspection measurements are schematically represented in Figure 3.

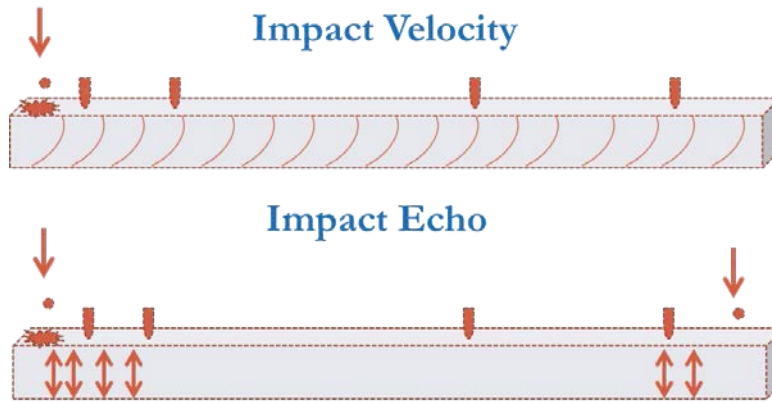


**Figure 3. IV and IE Measurements on Ties**

## **2.2 Union Pacific Railroad Prototype System Testing**

An evaluation of the inspection system was conducted at Union Pacific Railroad's (UP) Engineering Services, Inc. (ESI) facility in Omaha, NE, on October 21–23, 2012. Seventy-one ties at various stages of deterioration, ranging from new to falling apart, were tested using the device pictured in Figure 2. Each tie was marked with an identification number (1 to 71) and end direction (N-north end, S-south end). Visible exterior surface cracks were highlighted with red keel and ties with pulled pre-stressing wires labeled with a "P." Tie 2, south end, is shown in Figure 4.



**Figure 4. Tie 2, South, Showing Horizontal Crack**

Time domain data were used to determine PV compressional and shear wave arrival times, and a velocity was calculated using the sensor spacing. The PV data was used in two ways to rate each tie: 1) shear wave velocity values; and 2) an average dynamic strength calculation using compressional and shear wave velocity values. The results of this testing are shown in Figure 5.

Table-2 SUMMARY OF IMPACT VELOCITY AND ECHO RESULTS									
Tie ID	Observations				Impact Vel & Echo			Comments	Final
	Visible Cracks		Internal	Pulled	Thick	Comp.	Shear		Tie
Number	Top (inch)	Side (inch)	Cracks (inch)	Wires at end	Frq KHz	Vel ft/sec	Vel ft/sec		Rating
59-S	No top	48+	NA	yes	5.7	8500	1000	Spall top of tie	5
58-S	No top	30	NA	yes	none	8400	1000	Spall top of tie	5
44-S	21-30	30	NA	yes	3.27	13600	6600		4
45-N	28	30+	NA	no	none	13800	6400		5
8-S	14	30+	NA	yes	6.52	13400	5700		5
65-N	21	30	NA	yes	none	11900	6300		5
66-N	14	28	NA	yes	none	14500	6100		5
2-N	12	28	28+	yes	none	13400	6700		4
3-N	TD	28	NA	yes	6.57	14300	6800	End of tie spalled	4
1-S	none	28+	14-16	yes	6.68	13,600	6,900		4
60-N	10	21	NA	yes	6.72	14100	7000	center crack	4
68-N	8	21	NA	yes	none	14800	7000		4
47-N	8	21	NA	yes	none	14800	6800		4
67-N	6	21	NA	yes	none	15100	6900		4
4-N	4	21	NA	yes	none	14000	5400		5
61-N	none	18	NA	yes	7.46	14500	7400		3
70-S	none	18	NA	no	7.03	13100	6700		3
7-N	6	15	14-15	yes	6.76	14900	7000		4
69-N	13	12	14-15	yes	7.52	14500	7000		3
46-S	none	12	NA	yes	6.33	14400	7300		3
71-N	14	none	NA	yes	7.38	14500	7200		3
48-N	8	none	NA	no	none	15600	7300		3
5-N	none	none	NA	no	none	15400	7500		2
6-N	none	none	NA	no	7.96	15600	7400		2
9-N	none	none	NA	no	7.82	15700	7400		1
10-S	none	none	NA	no	8.05	14800	7700		1
11-N	TD	none	NA	no	7.82	15400	7700	Tamper Damage	1
12-S	none	none	NA	no	7.81	16100	8000		1
13-S	none	none	NA	no	8.05	15100	7900		1
14-S	none	none	NA	no	8.05	14800	7900		1
15-S	none	none	NA	no	7.69	14800	7800		1
16-S	none	none	NA	no	7.93	15100	7600		1
17-S	none	none	NA	no	8.05	15700	8000		1
18-N	none	none	NA	no	7.6	15600	7600		1
19-S	none	none	NA	no	8.05	15100	7500		1
20-S	none	none	NA	no	7.69	14900	8000		1

58-S  
59-S  
Top  
Spalled  
Off



2-N  
Top  
Cracking  
with  
Delam



1-S  
No top  
Cracking



69-N  
Internal  
Cracking



63-S  
64-S  
Tamper  
Damage





Table-2 SUMMARY OF IMPACT VELOCITY AND ECHO RESULTS									
Tie ID	Observations				Impact Vel & Echo			Comments	Final Tie Rating
	Visible Cracks		Internal	Pulled	Thick	Comp.	Shear		
	Top	Side	Cracks	Wires	Frq	Vel	Vel		
Number	(inch)	(inch)	(inch)	at end	KHz	ft/sec	ft/sec		
21-S	none	none	NA	no	8.29	14800	7900		1
22-S	none	none	NA	no	8.17	15200	7800		1
23-S	TD	none	NA	no	8.05	14900	7600	Tamper Damage	1
24-N	none	none	NA	no	7.8	15700	7700		2
25-N	none	none	NA	no	8.29	16100	8300		1
26-N	none	none	NA	no	8.05	15400	7600		1
27-N	none	none	NA	no	8.29	15400	7800		1
28-N	none	none	NA	no	8.29	15300	7900		1
29-S	none	none	NA	no	8.17	15300	7700		1
30-S	none	none	NA	no	8.05	14600	7500		1
31-S	none	none	NA	no	8.29	15300	8100		1
32-S	none	none	NA	no	7.81	14500	7600		1
33-S	none	none	NA	no	8.05	14900	7800		1
34-S	TD	none	NA	no	8.42	14800	8100	Tamper Damage	1
35-S	none	none	NA	no	8.05	13600	7600		1
36-S	TD	none	NA	no	8.29	15100	8100	Tamper Damage	1
37-S	none	none	NA	no	8.17	14500	7900		1
38-S	none	none	NA	no	8.17	14300	8000		1
39-S	none	none	NA	no	8.17	14400	7600		1
40-S	none	none	NA	no	7.93	15300	7500	new	1
41-S	none	none	NA	no	8.05	15200	7500	new	1
42-S	none	none	NA	no	8.05	15400	7800	new	1
43-S	none	none	NA	no	7.81	15000	7800	new	1
49-S	none	none	NA	no	8.42	14900	7600		1
50-S	none	none	NA	no	8.17	15300	7800		1
51-N	none	none	NA	no	8.17	15100	7600		1
52-N	none	none	NA	no	8.17	15300	7800		1
53-N	none	none	NA	no	8.17	15100	7700		1
54-N	none	none	NA	no	8.05	15300	7900		1
55-S	none	none	NA	no	none	14600	7600		1
56-N	none	none	NA	no	8.17	15700	7700		1
57-N	TD	none	NA	no	8.42	14800	7600	Tamper Damage	1
62-S	TD	none	NA	no	8.05	15200	7600		1
63-N	TD	none	NA	no	8.29	15600	7600	Tamper Damage	1
64-S	TD	none	NA	no	8.42	14100	7700	Tamper Damage	1

40-S  
41-S  
42-S  
43-S  
new  
ties



Pulled End  
(indented)  
Prestressing



**Grading Criteria**

- Grade Rating - 1  
Thickness Frq 7.5 to 8.5 KHz  
S vel. greater than 7,500 ft/sec
- Grade Rating - 2  
Thickness Frq 7.5 to 8.5 KHz  
S vel. less than 7,500 ft/sec
- Grade Rating - 3  
No 7.5 to 8.5 KHz Thickness Frq  
S vel. 7,000 to 7,500 ft/sec
- Grade Rating - 4  
No 7.5 to 8.5 KHz Thick Frq  
S vel. 6,500 to 7,000 ft/sec
- Grade Rating - 5  
No 7.5 to 8.5 KHz Thick Frq  
S vel. less than 6,500 ft/sec

**Figure 5. UP Tie Inspection Data and Grading**

### **2.2.1 Tie Dissection**

Based on the test results, six tie ends were dissected and the internal cracking patterns were mapped, as shown in Figure 6.



**Figure 6. Example of Internal Cracking**

Observations indicate that the pattern of crack propagation does not include cracking visible in the top surface until the side and cross-section cracks have progressed to a moderate stage of deterioration. The appearance of top cracks in a tie is an indication that the tie has significant internal cracking. The ties documented in this investigation demonstrate that by the time a crack is visible in the top chamfer and top surface to a length of several inches, the pattern of cracking along the sides of the tie and within the tie has progressed significantly. Appendix A contains a detailed report of the tie dissection activity.

### **2.2.2 UP Testing Conclusions**

A comparison of the observed internal cracking, the sonic nondestructive testing results, and UP visual tie rating was made to evaluate the effectiveness of nondestructive IV and IE measurements in rating concrete cross-ties. Comparison of visual distress with the actual extent of cracking present and IV and IE findings indicates that the in-service top surface visual inspection is far less capable of identifying ties in the early stages of cracking and deterioration compared to the nondestructive IV and IE measurements.

The combination of nondestructive PV and IE measurements can characterize internal cracking and can be used to condition rate concrete cross ties. Low or missing IE resonant frequencies are caused by internal cracking and delamination. PV values appear to be most influenced by the length of the internal cracking, becoming progressively lower with longer and cracks.

Based on the results of this investigation a Tie Rating Decision Tree was developed, illustrated in Figure 7.

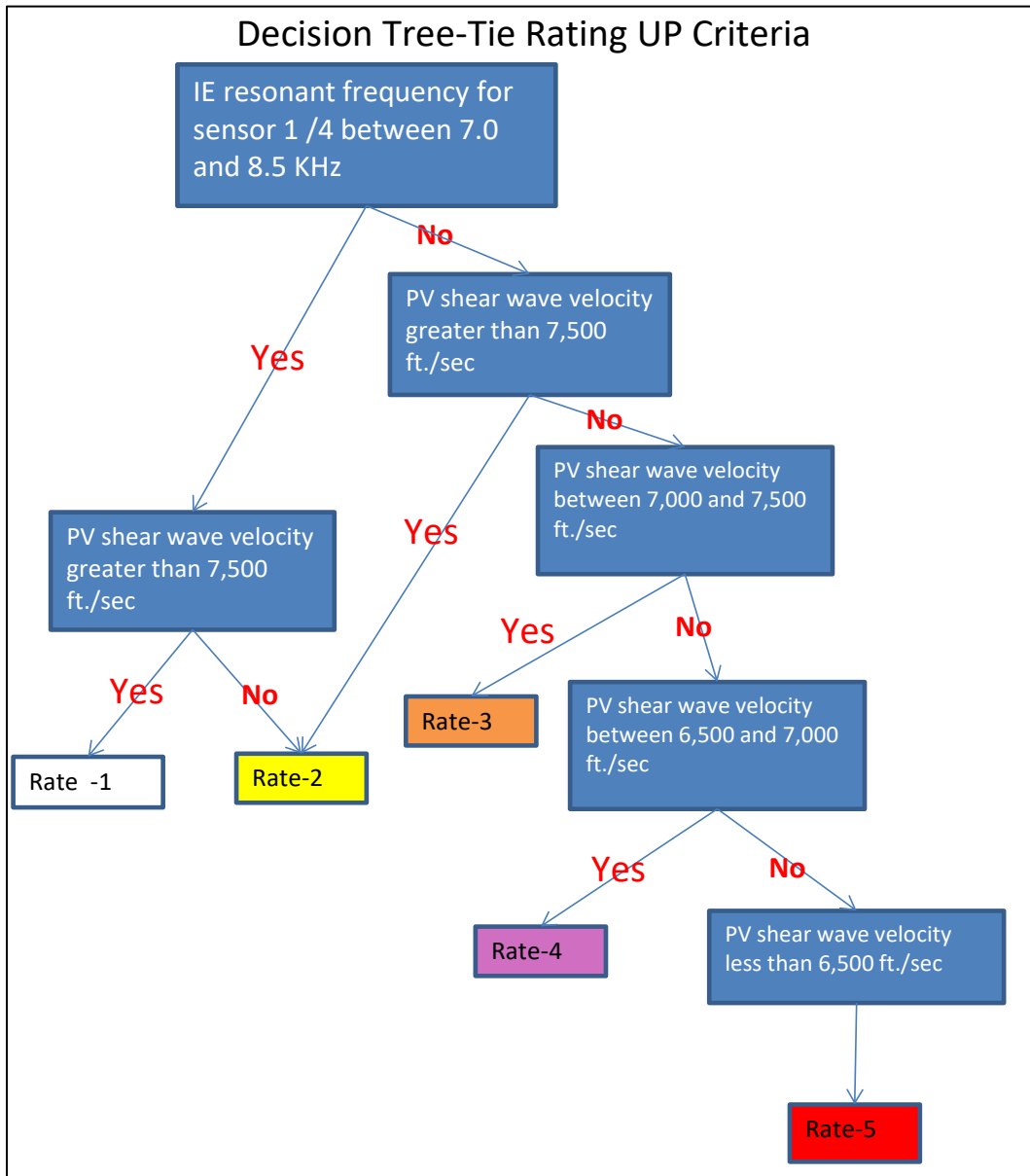


Figure 7. Tie Rating Decision Tree

### 2.3 Metro-North Railroad System Automation and Testing

To demonstrate that the IV and IE measurements can be made in a production mode, an on-rail ACTT-1 push carriage was built and tested, seen in Figure 8.





**Figure 8. ACTT-1 System on Metro-North Railroad**

The ACTT-1 device uses the same sensors and impact energy source as the handheld beam (Figure 2), but the instruments are mounted on a rolling cart to permit continuous testing. This system has eight sensors mounted on an axle so at every  $\frac{1}{2}$  rotation of the axle, four sensors are in contact with the tie. Sensors are positioned so that there is a sensor near each end of each tie and a sensor inside of each rail. The system is equipped with two projectile energy sources (one at the end of the tie) that are activated when the sensor comes in contact with the tie. There is a built in delay between the projectile energy sources to avoid interference between the tie end measurements.

NDT conducted proof-of-concept testing of the ACTT-1 system on Metro-North Railroad (Metro-North) tracks in March 21, 2013. Sixty ties were tested. The complete test report is included as Appendix B. The following summarizes the results:

- The ACTT-1 system acquired data at the rate of 1 tie per second.
- The data quality was similar to that obtained during the UP testing with the handheld beam. Resonance frequencies and compression and shear wave velocity data was adequate to rate the ties. All but four ties rated “1” using the tie rating decision tree developed during the UP testing (Figure 6).
- The presence of ballast did not appear to affect the data quality.

## 2.4 UP Automated Testing

NDT completed an evaluation of the use of nondestructive PV and IE testing to rate in-service concrete cross-ties along a section of UP's line between Central City and Clark, NE, on May 20–22, 2013. Ninety-one ties were tested.



**Figure 9. ACTT-1 System on UP Track**

The full test report is presented in Appendix C. The objectives for this test were:

1. To determine if sonic/ultrasonic IV and IE data are affected by ballast and attached rails.
2. To determine if ballast condition affects the results.
3. To compare automated results with the handheld device.

### 2.4.1 Testing Results

NDT tested the ACTT-1 system at two locations to obtain data from automated production. The objectives of these tests were to determine the quality of collected data and correlate results with visual inspected tie conditions. The purpose of a data quality check was to determine if there is any additional signal noise generated from the system or the surroundings that can cause degraded data quality. The data quality is adequate for evaluating tie conditions but could be quieter.

At the Clark “Mud Fouled Area,” UP tie numbers 529, 530, 531, 532 and 533 were tested with both the handheld beam and ACTT-1 systems. There was no noticeable difference in the data or rating for the ties that were in dry “good” ballast condition versus the ties that were partially submerged in wet silt filled ballast. These ties have resonant thickness frequencies at or near the

anticipated range of 7.5 to 8.5 kHz. Shear/Rayleigh wave velocity values are also in a range of 6,500 to 8,000 ft/sec, a range detected in previous testing.

Data were acquired on 16 ties with the hand held sensor array used in previous testing and with the ACTT-1 system. The measured thickness resonant frequency values and shear wave velocities acquired with the ACTT-1 system are within the reading error of the data of the handheld beam. Ten of the 16 ties were rated exactly the same and the other 6 were within 1 rating of each other.

### Clarks Mud Fouled Area Comparison

Tie	South Array Freq.	South Auto Freq.	North Array Freq.	North Auto Freq.	South Array Vel.	South Auto Vel.	North Array Vel.	North Auto Vel.	Array Rank	Auto Rank
520	7.38	7.45	7.67	7.42	7	7.93	7.28	7.20	Rank 3	Rank 3
521	7.38	7.55	7.67	7.93	7.13	7.33	7.4	7.09	Rank 3	Rank 2
522	7.52	7.58	7.67	7.83	7.5	7.57	7.5	7.38	Rank 1	Rank 2
523	7.52	7.7	7.67	7.67	7.2	7.41	7.51	7.26	Rank 2	Rank 2
524	7.52	7.59	7.74	7.6	7.29	7.41	7	7.29	Rank 2	Rank 2
525	6.57	8.05	7.67	7.73	7.38	1.82	7	7.00	Rank 3	Rank 2
526	7.6	7.71	7.6	7.73	7.38	8.03	7.66	7.23	Rank 2	Rank 2
527	8.05	7.82	7.6	7.67	7.43	7.57	7.43	7.17	Rank 2	Rank 2
528	7.6	8.39	7.82	7.82	7.36	7.33	7.11	7.50	Rank 2	Rank 2
529	8.13	7.97	7.74	7.9	7.38	7.54	7.64	7.38	Rank 2	Rank 2
530	8.05	8.13	7.82	7.82	7.22	7.59	7.22	7.17	Rank 2	Rank 2
531	8.05	7.31	7.67	7.67	7.31	7.5	7.3	7.50	Rank 2	Rank 3
532	8	8.21	7.82	7.82	7.55	7.54	7.26	7.29	Rank 2	Rank 2
533	8.13	8.13	7.97	7.97	7.36	7.66	7.44	7.41	Rank 2	Rank 2
534	7.5	7.52	7.82	7.74	7.16	7.66	7.17	7.79	Rank 2	Rank 1
535	7.82	7.9	7.9	7.82	7.58	7.66	7.58	7.44	Rank 1	Rank 2

**Figure 10. Handheld (Array) Versus Automatic Ranking**

#### Center Cracked Ties

Several ties with center cracking were tested. There was no significant drop in end to end wave velocity values with these ties. Close examination of some of these ties determined the center cracking, although extensive, does not extend the full thickness of the tie. Cracking did not propagate into the pre-stressed region of the tie, therefore, it is unlikely that IV data with the sensor spacing used for this testing will detect this cracking.





**Figure 11. UP Ties with Center Cracking**

## **2.5 UP Repeatability Testing**

NDT conducted sonic/ultrasonic IV and IE testing of pre-stressed concrete railroad cross-ties along a section of UP's line between Central City and Clark, NE, on October 2, 2013. Testing was conducted over a distance of approximately ¼ mile (633 ties), while data were acquired on two runs over the same ties to evaluate the repeatability of the results.

Sonic/ultrasonic data was acquired with the automated concrete tie (ACT) system developed by NDT. The ties tested were CXT concrete ties that were inspected, while deficient ties were replaced within the last 6 months.

Appendix D contains the full data set. The results show that the ACTT-1 test is very repeatable. The results of the IV and IE testing indicates that 99.9 percent of the ties have a rating of #1 or #2 and none of the ties have full thickness center cracking. The difference between a #1 and #2 rating is not very significant, in both cases the data is indicating concrete in compression (pre-stressing wires have not slipped), with minor (micro) cracking which would be expected for ties that have been inspected, while deficient ties are replaced within the last 6 months. A comparison of the results (overall rating) between run 1 and run 2 indicates 150 of the 263 ties tested or 57 percent of the ties have exactly the same overall rating. Some of the data differences are due to no velocity data on sensor 2. It was observed during data acquisition that the gauge on the Nolan cart wheels is not close enough to the rail gauge resulting in the cart moving laterally and sensors not in contact with the tie. It was also observed that the sensor axle drive wheel's circumference is greater than 2 feet resulting in the need to correct the sensor position every 10 to 15 ties.

## **2.6 Phase 1 – Conclusions**

The IV and IE technique is proven effective at measuring the internal condition of concrete crossties in both handheld beam and automated cart (ACTT-1) configurations. A five category rating system was developed and corresponds well to railroad inspector ratings

Shear wave velocity appears to be the best data to use for tie rating. The IE frequency data can indicate if there is little to no end cracking but, if cracking is present, the resonant thickness frequencies are not detected. Compressional PV data can be influenced by water saturation. Shear wave data are not affected by water saturation and velocity values can be used to rate the cracking severity. The system is not sensitive to the presence of rails or the ballast condition. Also, the system does not detect center tie cracking where the cracks do not propagate into the pre-stressing steel matrix.

The ACTT-1 production mode testing system can accurately test ties at a rate of 1 tie every 2 seconds (1,800 ties per hour or about 0.7 mph). Skewed ties due to tamping and unevenly spaced ties are the primary hindrance to faster testing rates. Ties on curves are only slightly cantered and did not pose a problem for production testing. Improvements to the sensor drive mechanism should increase this production rate to 1 tie per second, 3,600 ties or 1.4 mph.

### 3. Phase 2 – Production Prototype Development and Demonstration

This section of the report covers the activities of Phase 2, which focused on developing and testing an automated method to test ties in track from a moving platform.

#### 3.1 Scope

Phase 2 continued the research effort to meet specific objectives to improve the efficiency of concrete tie testing, and progress the inspection technology to a production prototype level through automation, which included the following:

1. An evaluation of the use of non-contact microphone sensors and other energy sources.
2. The improvement of the manual prototype system to use tie clips to locate sensors and the energy source near the middle of the tie.
3. The Development data acquisition software that can instantaneously evaluate, rate/rank and mark ties.
4. The acquisition of on-rail data to evaluate production rates and develop a data base of comparison between tie conditions and IVE data.

#### 3.2 Microphone Sensors

Contact sensors are typically used to record wave arrivals, but they can be difficult and slow to use due to tie spacing variables. Rayleigh waves produce sound as they propagate through concrete that can be detected by common microphones [3]. The use of microphone sensors would simplify and accelerate data acquisition.

Measurements were made with a microphone positioned beside a piezo ceramic contact sensor using a projectile impact. A direct comparison of the wave arrivals was made to determine if the Rayleigh wave arrivals detected by the microphones have the same velocity as the contact sensor (Figure 12). The results show that a microphone can be used in place of a contact sensor.

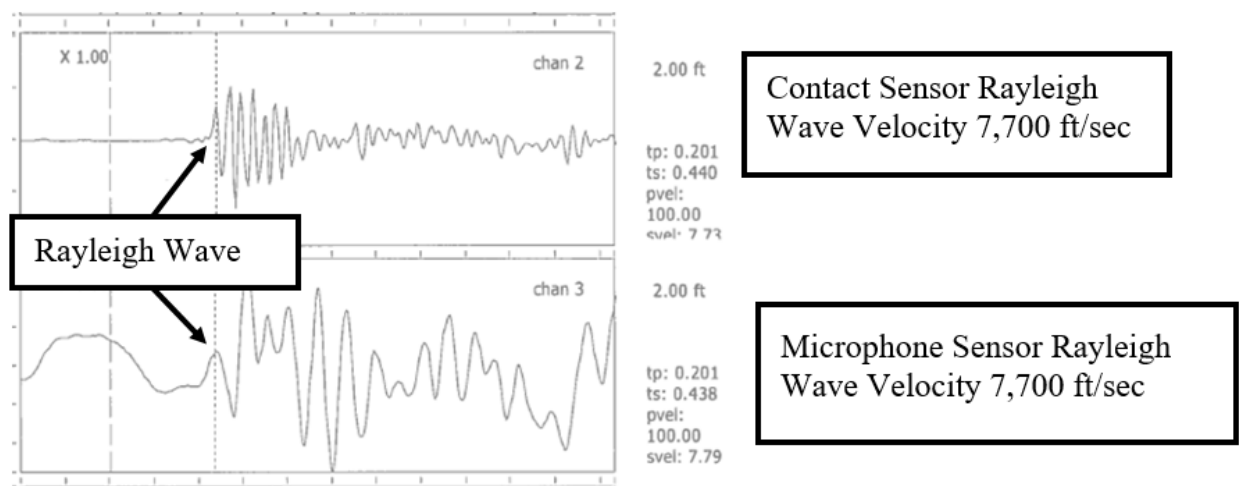
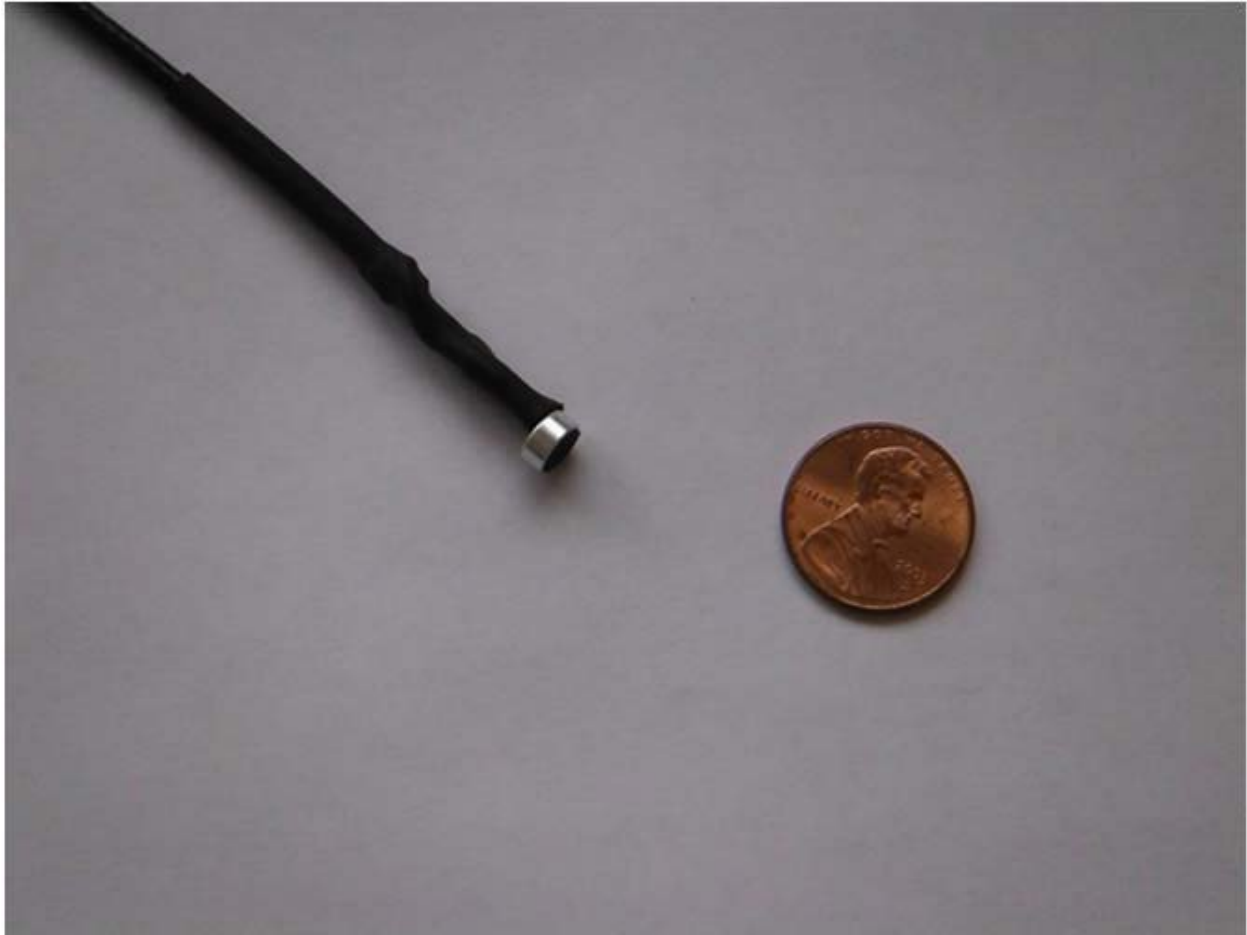


Figure 12. Comparison of IV Data Recorded with Contact and Microphone Sensors

Literature indicates that microphone sensors with a center frequency of approximately 20 KHz are best for detecting Rayleigh waves. Several microphones were evaluated and it was

determined that a microphone with a center frequency of 17 KHz with a sensitivity of -58 DBV/microbar and noise cancelling worked best. These microphones are small and readily available.



**Figure 13. Microphone Sensor**

Testing determined that microphones mounted in a shotgun configuration work best. A shotgun configuration mounts the microphone in a tube so that the source of the sound detected by the microphone is projecting from one direction (Figure 14). Numerous experiments were conducted varying the distance of the microphone from the end of the shotgun tube opening and the distance the microphone was mounted in the tube. The results indicate that a ½ inch PVC tube with the microphone positioned approximately 3 inches inside the shotgun tube and approximately 2 inches above the surface of a concrete crosstie yields better results.



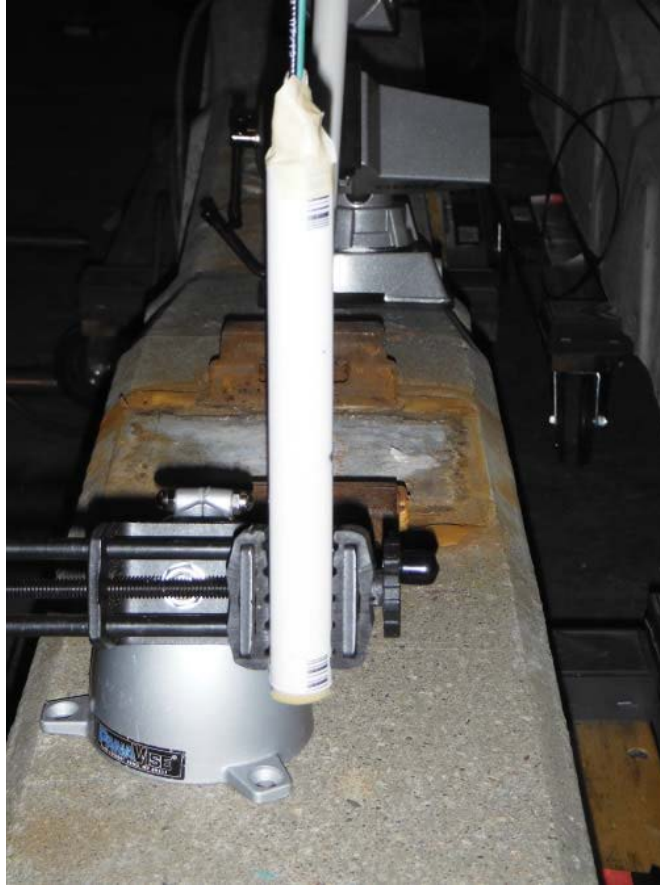


**Figure 14. Shotgun Microphone Mount**

### **3.2.1 *Triggering and System Testing***

The microphone is used as a trigger sensor for data acquisition. Background noise is a concern when using a microphone, as spurious background noises could trigger the data collection process. NDT conducted experiments to test for the effects of background noise using a radio at high volume with static to simulate high frequency noise, and drums to simulate low frequency noise. The noise did not appear to have any significant effect on the data. Using microphones exhibited an unanticipated finding that the crosstie resonance thickness (IE) was strong and at the same frequency as the contact sensor.

NDT performed an additional test to compare the performance of microphones to piezo ceramic contact sensors. This data was used to evaluate the automatic data interpretation software and to make a comparison between contact sensor data and data acquired with the moving microphone tapper data acquisition system. Figure 15 is showing the comparison of data performance between microphones and piezo ceramic contact sensors. The microphone velocity values were determined with the automatic pick data and the piezo ceramic data were read manually by a technician. There is no significant difference between the readings. Figure 16 is showing the data from a repeatability test of the microphone system. System repeatability is acceptable.

Table -3 Comparison Microphone and Contact Sensor Velocity Values									
Left Side					Right Side				
Tie #	shot #	micro Vs	Con Vs	diff	Tie #	shot	Micro Vs	Con Vs	diff
50	1	7.64	7.48	0.16	50	1	7.55	7.92	-0.37
51	2	7.54	7.21	0.33	51	2	7.01	6.98	0.03
52	3	8.02	7.01	1.01	52	3	7.01	7.23	-0.22
53	4	7.71	7.48	0.23	53	4	8.15	7.47	0.68
54	5	7.4	7.21	0.19	54	5	7.18	7.56	-0.38
55	6	7.3	7.44	-0.14	55	6	7.07	7.38	-0.31
56	7	7.62	7.44	0.18	56	7	7.01	7.53	-0.52
57	8	7.6	6.99	0.61	57	8	7.35	7.12	0.23
58	9	7.82	7.73	0.09	58	9	7.22	7.32	-0.1
59	10	7.9	7.25	0.65	59	10	7.25	6.88	0.37
60	11	7.6	7.37	0.23	60	11	7.14	7.21	-0.07
61	12	7.9	7.32	0.58	61	12	7.39	7.47	-0.08
62	13	7.57	7.73	-0.16	62	13	5.84	7.26	-1.42
63	14	7.58	7.5	0.08	63	14	7.43	6.93	0.5
64	15	7.52	7.04	0.48	64	15	7.24	7.2	0.04
65	16	8.27	7.46	0.81	65	16	7.45	7.47	-0.02
66	17	7.72	7.37	0.35	66	17	7.36	7.38	-0.02
67	18	7.93	7.58	0.35	67	18	7.53	7.44	0.09
68	19	7.93	5.35	2.58	68	19	7.53	7.26	0.27
69	20	7.76	7.53	0.23	69	20	7.57	7.38	0.19
70	21	7.77	7.32	0.45	70	21	7.35	7.27	0.08
71	22	7.67	7.56	0.11	71	22	7.29	5.93	1.36
72	23	7.29	7.08	0.21	72	23	7.41	7.58	-0.17
73	24	7.57	7.46	0.11	73	24	7.55	7.43	0.12
74	25	7.96	7.27	0.69	74	25	7.44	7.27	0.17
75	26	7.01			75	26	7.76	7.45	0.31

Vs=Rayleigh Wave Velocity values X 1000 ft/sec

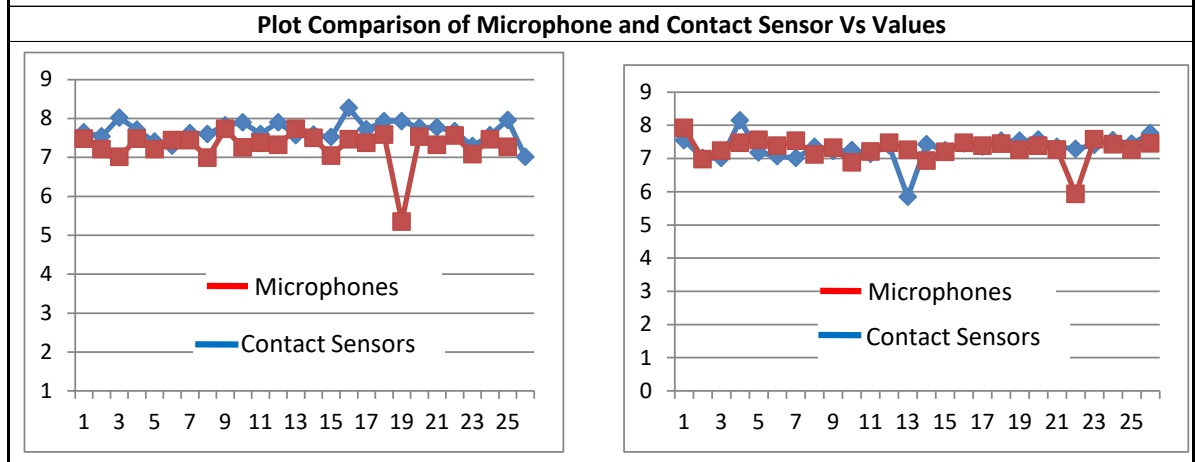


**Figure 15. Shotgun Microphone Versus Contact Sensors**

Table-4 Comparison Run 1 & 2 Microphones Rayleigh Wave Velocity Values										
Left Side Microphones					Right Side Microphones					
Tie #	shot	Run 1 Vs ch2	Run 2 Vs ch2	diff	Tie#	shot	Run 1 Vs ch2	Run 2 Vs ch2	diff	
50	1	6.83	7.64	-0.81	50	1	7.47	7.55	-0.08	
51	2	7.13	7.54	-0.41	51	2	7.01	7.01	0	
52	3	7.13	8.02	-0.89	52	3	7.01	7.01	0	
53	4	7.18	7.71	-0.53	53	4	8.33	8.15	0.18	
54	5	7.01	7.4	-0.39	54	5	7.38	7.18	0.2	
55	6	7.22	7.3	-0.08	55	6	7.11	7.07	0.04	
56	7	7.15	7.62	-0.47	56	7	7.24	7.01	0.23	
57	8	7.01	7.6	-0.59	57	8	7.33	7.35	-0.02	
58	9	7.01	7.82	-0.81	58	9	7.14	7.22	-0.08	
59	10	6.86	7.9	-1.04	59	10	7.37	7.25	0.12	
60	11	7.37	7.6	-0.23	60	11	7.24	7.14	0.1	
61	12	7.2	7.9	-0.7	61	12	7.14	7.39	-0.25	
62	13	7.41	7.57	-0.16	62	13	7.08	5.84	1.24	
63	14	7.66	7.58	0.08	63	14	7.24	7.43	-0.19	
64	15	7.7	7.52	0.18	64	15	7.32	7.24	0.08	
65	16	7.85	8.27	-0.42	65	16	7.52	7.45	0.07	
66	17	7.99	7.72	0.27	66	17	7.62	7.36	0.26	
67	18	7.62	7.93	-0.31	67	18	7.57	7.53	0.04	
68	19	7.29	7.93	-0.64	68	19	7.48	7.53	-0.05	
69	20	7.87	7.76	0.11	69	20	7.57	7.57	0	
70	21	8.05	7.77	0.28	70	21	7.01	7.35	-0.34	
71	22	7.76	7.67	0.09	71	22	7.01	7.29	-0.28	
72	23	7.84	7.29	0.55	72	23	7.01	7.41	-0.4	
73	24	7.99	7.57	0.42	73	24	7.32	7.55	-0.23	
74	25	8.09	7.96	0.13	74	25	7.68	7.44	0.24	

Vs = Rayleigh wave Velocity X 1000 ft/sec

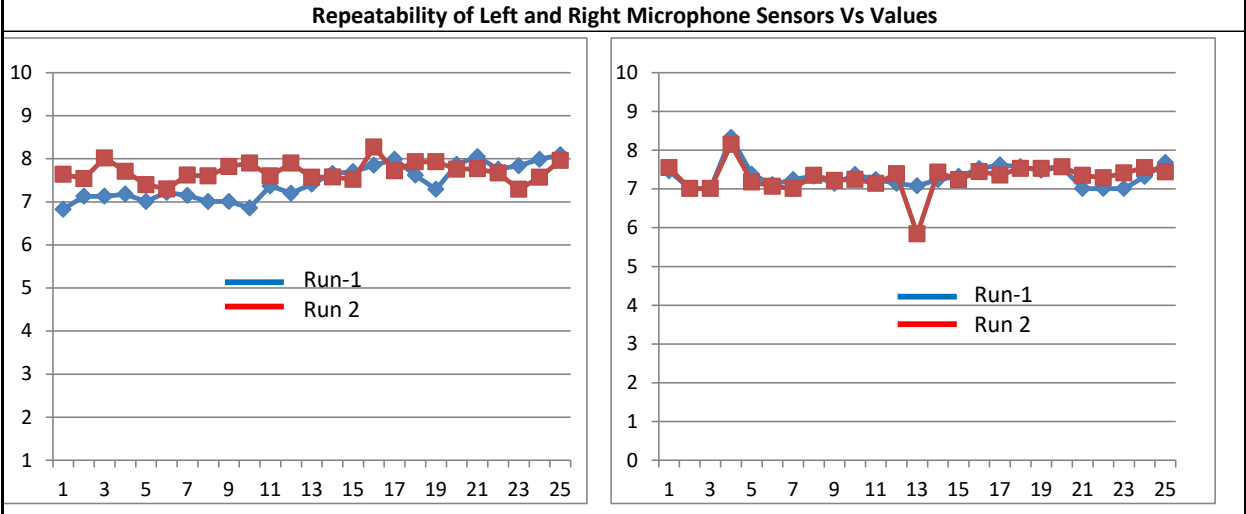


**Figure 16. Microphone System Repeatability Test Results**

### 3.3 Alternate Energy and Wave Generation System

The ACTT-1 and the handheld beam systems used an air fired projectile (small sphere) device to impart wave energy to the tie. This device functioned well, but required a compressed air power source and the spheres were not contained. The rebounding spheres posed a safety concern.

NDT explored the use of alternative energy sources, including a spring activated point source similar to a center punch used in machine shops, a metal ball on a metal arm to create a glancing impact, an electric solenoid, a bar drop impactor, and a projectile impact where the projectile is captured so it cannot fly away and cause damage. All testing used microphones in a shotgun configuration.

The machine shop center punch produced a reasonably good Rayleigh wave signal, but with use the wear on the spring made the signal character inconsistent. Electric and pneumatic vertical solenoids produced a lower frequency signal but the Rayleigh wave could not be read accurately. Another operational drawback of the vertical solenoid is it did not rebound or retract and in a moving operation would drag along the crosstie surface creating a noisy signal and difficulty reading Rayleigh wave arrivals.

Several experiments were conducted to emulate a rod impact that would rebound and be captured with a magnet (reusable impactor). A nail gun with a small finish nail produces a weak noisy signal. Using a tube as a guide and free falling rods produced a good signal, but the free-falling rod was not predictable.

Figure 17 provides an image of a set of impactors that were tested and found to produce a sharp, clean, reproducible signal. The small diameter (1/8) impactors did not have enough energy to produce a good signal and were difficult to work with. The large diameter balls produced a strong signal, but also produced spurious frequencies. The middle-sized impactors (3/8" and 5/16") had the best results.



**Figure 17. Ball End Impactors**

An impactor (“tapper”) with a 3/8 diameter ball was mounted on a rotational solenoid and was found to be an ideal energy sources, as seen in Figure 18.



**Figure 18. Ball End “Tapper” Installed on ACTT-2**

### **3.4 Improved Tie Locator**

Crossties that are misaligned or are not spaced evenly contribute to slowing data acquisition due to the system having to stop while the sensors realign with the crosstie. A magnetic proximity switch with an Arduino controller programed to activate the solenoid when it passes by a rail clips was determined to be a reasonable solution to positioning microphones and “tapper” energy source on each crosstie. The magnetic proximity switch, Arduino controller and rotational solenoid impactors were mounted on the ACTT-2 system and tested on-rail, as shown in Figure 19. The proximity switch with an Arduino controller system works reliably for speed of 3 to 5 mph and probably much higher.





**Figure 19. Magnetic Proximity Switch Installed on ACTT-2**

### **3.5 Software Development**

NDT developed software to analyze the IV data and grade ties in real-time. The software was developed in three stages.

Stage 1 was a data acquisition program that acquired, archived and displayed the microphone data. This program obtained data from two separate sensor arrays spaced 1 foot apart, acquiring data at opposite ends of adjacent cross-ties. Each array is triggered by a proximity switch activated when the ACTT-2 system moves past the rail clips. The program was written so that if data were not acquired (missed) on two consecutive ends, then an audible alarm would be sounded with a visual display.

Stage 2 was software used to interpret the data as it was being acquired. This software establishes a zero time, the instant the Rayleigh waves pass the microphone sensor closest to the taper impact energy sources, and the time for the signal to propagate to microphone 2 inside the rail and sensor 3 next to the opposite rail. The distances between sensors are known, therefore, the measured times can be used to calculate the average Rayleigh wave velocity. The velocity

values measured independently at each end of the crosstie are compared and the lower value is used in the decision tree, as seen in Figure 20, to rank or grade the crosstie.

Stage 3 was to write software to activate a paint spray mechanism to mark crosstie rate/grade 3, 4 or 5 (weak, fractured delaminated crossties).

Software was tested during several visits and on-rail testing was conducted at the RED Transfer & Logistics facility in Portland, CT.

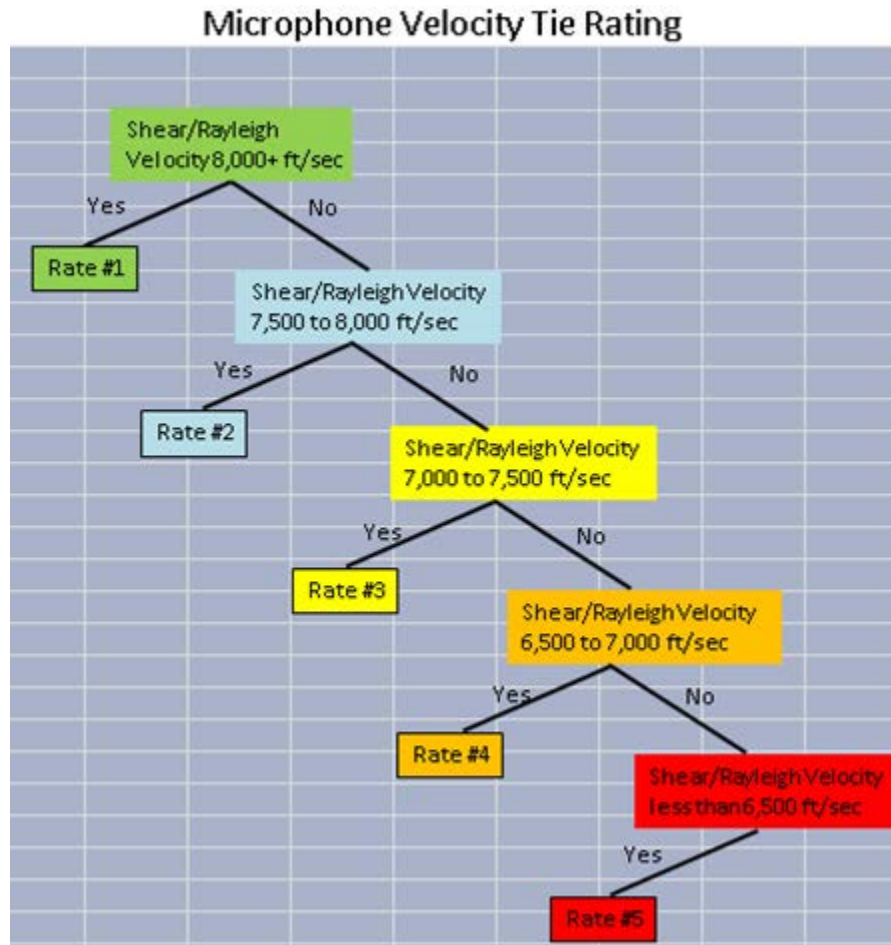


Figure 20. Rayleigh Wave Velocity Decision Tree for Rating Ties

### 3.6 ACTT-2 System and Testing

NDT built a new light weight carriage system utilizing the proximity switches, microphone sensors, “tapper” energy sources, and an on board computer to process data.





**Figure 21. ACTT-2 System On-Rail and Folded for Transport**

### **3.7 System Testing and Demonstration**

The ACTT-2 system was tested several times at the RED Transfer & Logistics facility in Portland, CT. The first tests were to evaluate the mechanical operation of the ACTT-2. The findings of this testing are listed below:

- The polyurethane wheels are very quiet.

- The magnetic proximity switch, Arduino and solenoid impactor work well up to 3 mph.
- The entire system can be rotated or removed from rail by two men.

The microphone data acquired during this test was interpreted to rate each crosstie from 1 to 5 using the decision tree (Figure 20). A visual inspection using Amtrak’s “Concrete Tie Condition Evaluation & Safety Inspection Procedure” was made and the results were compared with the microphone rating data (Figure 22). This data indicates a reasonable comparison of results, given that the visual inspection only shows a limited area of the crossties.

Tie #	Visual Rating	Microphne Vel Rating	Difference
50	2	2	0
51	2	3	-1
52	3	3	0
53	3	2	1
54	3	3	0
55	3	3	0
56	3	3	0
57	3	3	0
58	2	3	-1
59	3	3	0
60	2	3	-1
61	3	3	0
62	2	4	-2
63	2	3	-1
64	3	3	0
65	3	3	0
66	3	3	0
67	2	2	0
68	2	2	0
69	3	2	1
70	2	3	-1
71	3	3	0
72	3	3	0
73	3	2	1
74	3	3	0
75	3	3	0

**Figure 22. ACTT-2 Test Results**

The ACTT-2 systems was demonstrated at the TTC in Pueblo, CO, on March 29–30, 2016. This demonstration resulted in two improvements to the ACTT-2 system:

1. Butterfly rail clips resulted in two energy taps on each tie. The magnetic proximity switch was modified with an option to add an additional magnetic proximity switch to produce one energy tap when butterfly rail clips are present.
2. Tappers were mounted on a single support strut. As a result, one tapper was striking with the solenoid behind the ball which resulted in the ball dragging on the tie surface as it

rebounded. A second strut was added so that the ball taper is trailing the solenoid. It is hoped that this modification will result in higher data acquisition rates.



**Figure 23. ACTT-2 Demonstration at the TTC**

NDT also demonstrated the system during at the June 15, 2016, International Crosstie and Fastening System Symposium at the University of Illinois.





**Figure 24. ACTT-2 Demonstration at the 2016 International Crosstie and Fastener Symposium, Urbana, IL**

## 4. Conclusion

---

The NDT Corporation developed a non-destructive system used to quantify the internal concrete crosstie conditions and accurately rate tie conditions. The data compares favorably with existing visual tie grading methods. The results of this investigation demonstrated that:

1. The horizontal cracking and delamination typically hidden from view in ballast are readily indicated by IV Rayleigh wave velocity values.
2. The severity of cracking and length (distance from the end) of internal cracks can be categorized based on Rayleigh wave velocity values.
3. The data collected from the ACTT system compares favorably to the grading criteria used by several railroads.

System development and testing has shown that IV Rayleigh wave data can be acquired in a systematic production manner in real-time and can accurately evaluate ties for internal cracking and deterioration. Currently, production data acquisition rates are approximately 2 to 3 mph, but it is believed that these rates can be increased significantly with adjustments to the “tapper” energy source. Time over tie calculations indicate the microphone sensor could collect data at a speed in excess of 20 mph.

A high-rail mounted system and a portable backpack system were proposed, but not developed. The carriage mounted system (ACTT-2) can be easily modified to be mounted on a high-rail vehicle, but it is unclear if the system can obtain high quality data at speeds that high-rail vehicles can travel. Future testing will determine if the system can operate at speeds of 10 or 20 mph. Due to the microphones being smaller in size, a handheld tapper can be used, however, a portable backpack system is feasible.

## 5. References

---

1. ASTM C597-09. (2009). “Standard Test Method for Pulse Velocity Through Concrete.” ASTM International: West Conshohocken, PA. Available at: <https://www.astm.org/>.
2. ASTM C1383-15. (2015). “Standard Testing Method for Measuring the P-Wave Speed and the Thickness of Concrete Plates Using the Impact-Echo Method.” ASTM International: West Conshohocken, PA. Available at: <https://www.astm.org/>.
3. ASTM C666/C666M-1503. (2015). “Standard Testing Method for Resistance of Concrete to Rapid Freezing and Thawing.” ASTM International: West Conshohocken, PA: Available at: <https://www.astm.org/>.
4. Al Wardany, R., Rhazi, J., Ballivy, G., Gallias, J. L., and Saleh, K. (n.d). “Use of Rayleigh Wave Methods to Detect Near Surface Concrete Damage.” Research Group on NDT and Instrumentation, Université de Sherbrooke: Sherbrook, Canada. Available at: [http://www.ndt.net/article/wcndt2004/html/htmltxt/729\\_wardany.htm](http://www.ndt.net/article/wcndt2004/html/htmltxt/729_wardany.htm).
5. Bjurström, H. (2014, November 14). “Air-Coupled microphone measurements of guided waves in concrete plates.” KTH Royal Institute of Technology, Engineering Sciences: Stockholm, Sweden. Available at: <https://www.diva-portal.org/smash/get/diva2:763348/FULLTEXT01.pdf>.

# Appendix A: Union Pacific Test Results – October 2012

---

## REPORT OF FINDINGS:

### INVESTIGATION OF CRACKING PATTERNS IN PRESTRESSED CONCRETE RAILROAD TIES

#### CONDUCTED:

UNION PACIFIC/ ENGINEERING SERVICES, INC.  
OMAHA, NEBRASKA

#### CONDUCTED FOR AND IN ASSOCIATION WITH:

NDT CORPORATION  
STERLING, MASSACHUSETTS

---

## INTRODUCTION

Lewis Engineering and Consulting, Inc. (LEC), Gainesville, Florida was requested by NDT Corporation, (NDT) Sterling, Massachusetts to participate in the investigation of prestressed concrete railroad tie cracking and deterioration. NDT specializes in the application of impact echo acoustic non-destructive testing methods to investigate a wide variety of prestressed and post-tensioned concrete structures and structural components. The scope of the investigation was to identify cracking patterns in serially sectioned cross-sections of concrete railroad ties that had been investigated and rated with respect to degree of deterioration using the NDT impact echo methodology.

A site visit was made by both LEC to Union Pacific (UP) research and testing facilities at the Engineering Services, Inc. (ESI) office in Omaha, Nebraska, October 23-24, 2012. NDT personnel arrived earlier in the week to conduct preliminary impact echo tests on concrete railroad ties in various stages of cracking and deterioration that had been removed from service and stored at the UP/ESI facility. UP personnel provided their visual assessment rating of the available ties based upon the standard in-service, top-of-tie visual rating to compare with the NDT impact echo results.

Ties were selected serial sectioning with the objective of evaluating ties ranging from a visual scale of 1 to 5 and which had been evaluated via impact echo and assigned a corresponding condition rating of 1 to 5 based upon those findings. The objective of the destructive testing procedure was to create a series of cross-sections by saw cutting through the ties at increasing distances from the end towards the rail pad. The saw cut surfaces were then smoothed as necessary to allow visual identification of any cracks that were present. Cracks were made visible by spraying the cut surface with a mist of isopropyl alcohol. The alcohol

LEWIS ENGINEERING AND CONSULTING, INC.

would penetrate any cracks present and providing an visible indicator as the alcohol evaporated from the exposed surface of the tie. A red Sharpie marker was then used to outline any visible cracks. Photographs were recorded of the outlined tie cross-sections which are attached to the report in captioned figure pages.

Also documented and recorded was the depth-of- retreat of the prestressing wires at the ends of the ties prior to sectioning. The wire depth-of-retreat data are presented in **Appendix A**.

### **DESTRUCTIVE TESTING RESULTS**

NDT selected ties for dissection on the basis of evaluating at least one tie end that represented the visual and impact echo response rating within the range between 1 and 5, 5 being the worst condition. The results are presented in the order in which the ties were sectioned and documented.

#### **NDT TIE # 7, North End Rated Condition 5 by NDT**

**Figure 1** shows an overall view of NDT Tie #7, north end at right. Cast in place identification markings indicate that this tie was manufactured by CXT at Grand Isle, Nebraska in 2006 (G1439 6). Other markings visible are #455-D and 50? S.

The NDT transducer array is shown in **Figure 2** positioned as it was employed in recorded the impact echo response. Note in **Figure 3** that the transducer shown is located 8 inches from the end of the tie and closest to the impact location at nominally 2 inches from the end.

The top surface of Tie NDT #7 at the north end is shown in **Figure 4**. Note there is a crack outlined in red approximately 6 inches in length and spalling of concrete on one side. The pad and rail towers at the north end are shown in **Figure 5**. One readily visible crack and a pattern of retreat of the ends of the wires is evident in the end view in **Figure 6**. Side views of the north end are shown in **Figures 7 through 10**.

Prior to serial sectioning of the tie, all of the visible cracks were outlined in red as shown in **Figure 11**. Oblique end/side views in **Figures 12 and 13** show continuation of two of the primary end cracks down the sides of the tie. Saw cuts were made at 4 inches, 14 inches and 21 inches (center of pad) from the end. Cracks exposed at each serial cross-section face were



marked in red. The three cross-sections are shown together in **Figure 14**. The primary end cracks visible in **Figure 11** remain present in the 4 inch cross-section. At 14 inches from the end, the largest crack on the right hand side connecting the two wires at the upper right hand corner and the continuing side crack remains. Note that in both the 4 inch and 14 inch cross-sections that wire on the far right in the second row of wires from the top is displaced upward and closer to the top row right hand side wire than it should be. All other wires appear to be symmetrically spaced and in their correct locations.

At the 21 inch cross-section from the end, through the center of the rail pad, none of the cracks remain visible. This cross-section distance is beyond the 15 inch long crack that was outlined on the right hand side of the tie.

#### NDT TIE # 7, South End Rated Condition 1 by NDT

The top surface at the south end of tie NDT #7 is shown in **Figure 15**. Some spalling is visible over 6 inches inboard from the end and adjacent to the rail pad on one side. The rail pad is shown in **Figure 16**. The end of the tie without visible cracks outlined is shown in **Figure 17**. One side of the tie at the south end is shown in **Figures 18 and 19**; the opposite side is shown in **Figures 20 and 21**.

The serial sections removed at 4 inches and 8 inches are shown in an oblique end view from one side in **Figure 22** and from the opposite side in **Figure 23**. The continuation of the cracks outlined in red at the south end and along the sides are evident in the repositioned cross-sections. Much of the cracking visible in the end remains in the cross-section at the 4 inch cut as shown in **Figure 24**. However, none of the end or side cracking remains in the cross-section at 8 inches. The cast-in-place identification for tie NDT #7 is shown in **Figure 25**.

#### NDT Tie #69, North End Rated Condition 2 by NDT

An overall view of one side of tie NDT #69 is shown in **Figure 26** with the transducer array placed as it was employed in the impact echo tests. The north end is shown in **Figure 27** with all visible cracks outlined in red. Oblique end side views in **Figures 28 and 29** show the translation of end cracks into horizontal cracks along the sides and a crack in the top surface.

Cross-sections were removed at 4 inches, 8 inches and 14 inches from the end. The end, the 4 inch and 8 inch cross-sections with visible cracks outline in red are shown in the composite

image in **Figure 30**. It is apparent that crack progression diminishes with distance inboard from the end, but generally it is the upper two rows of four wires each where the cracks are most persistent and which intersect the horizontal cracks along the sides. The cross-section at 14 inches from the end contained no visible cracks as shown in **Figure 31**. Oblique end side views of the three removed sections aligned adjacent to each other showing the progression of the cracks in each cross-section are shown in **Figures 32 and 33**. A top view of all three pieces and the remainder of the tie is shown in **Figure 34**.

NDT Tie #69, South End Rated Condition 2 by NDT

The pattern of cracking present in the south end of tie NDT #69 is shown in an end view in **Figure 35** and oblique end side views in **Figures 36 and 37**. No cross-sections were removed from this end of the tie based upon the cracking similarity to the north end of the tie.

The date plug was removed from the tie identification location but the information was found illegible. Visible cast-in-place identification included "505S" and "357-D."

NDT Tie #2, North End Rated Condition 4 by NDT

Side views of the north end of tie NDT #2 are shown in **Figures 38 and 39**. Horizontal cracks in both sides extend past the rail pads as indicated by red marker outlining the visible cracks. Significant spalling is also present at the upper end surface as shown in **Figure 38** and the end view in **Figure 40**. The top surface at the north end is shown in **Figure 41**.

Due to the extent of spalling, the first cross-section removed was at 6 inches from the end. Oblique end side views of visible outlined cracks in that cross-section and the intersecting horizontal side cracks are shown in **Figures 42 and 43**. A similar pair of oblique end side views are shown in **Figures 44 and 45** after removal of a section at 10 inches from the end. The majority of the cracking visible at 6 inches from the end remains. A third cross-section cut was made at 21 inches from the end in the center of the tie pad. Two oblique end side views at that cross-section in **Figures 46 and 47** confirm the continuation of the internal cracking and intersection with the continuing horizontal side cracks.

A composite image in **Figure 48** shows the 6 inch section, the 10 inch section and the 21 inch section. A tower is being held in place at the top surface of the tie to show the location of the embed posts in that area of the tie relative to the top row of prestressing wire and the cracks

outlined in the face of the cross-section. A fourth and final cut was made 28 ½ inches from the end of the tie inboard of the inner rail tower. Cracking along one side remains visible at that distance into the tie from the end and within the cross-section surface as shown in **Figure 49**.

NDT Tie #2, South End Rated Condition 2 by NDT

There is no visible cracking present in the top surface and chamfered edges in **Figure 50** which would by visual in-service inspection would rate this end of the tie a "1." However, horizontal cracking is clearly evident along the both sides of the tie in **Figures 51 and 52**. These cracks would be obscured by ballast under in-service conditions. The end of the tie in **Figure 53** shows visible cracks outlined in red.

A composite image in **Figure 54** shows cross-sections and outlined cracks at 4 inches, 8 inches and 14 inches from the end of the tie. At the south end of tie NDT #2, cracks are present interconnecting the upper row of prestressing wires and the horizontal cracks along the sides which align with the second row of wires from the top. The south end of this tie represents a clear pattern of the mid-stage of crack growth at the end interconnecting with horizontal cracks along both sides of the tie but none of which would be evident in a visual in-service inspection.

The CXT identification markings on this tie include "505S", "357-A", and beneath the date plug "G1041" and "6" indicating 2006.

NDT Tie #1, South End Rated Condition 3 by NDT

The south end of this tie had no visible cracks on the upper surface and would have been rated condition "1" by a visual in-service inspection. An overall view of this tie is shown in **Figure 55**. The top surface shown in **Figure 56** contains no visible cracks. Horizontal cracks were present along the sides, however, to a distance of 21 inches from the end on one side in **Figure 57** and to 13 inches from the end on the opposite side shown in **Figure 58**.

The end of the tie with cracks outlined in red is shown in **Figure 59**. An oblique end view after removal of a cross-section at 4 inches from the end is shown in **Figure 60**. An opposite side oblique end view shows the alignment of the crack on the right side of the cross-section with the horizontal crack in the side. A second set of oblique end views in **Figures 62 and 63** show cracks remaining in a cross-section at 8 inches from the end of the tie. A third cross-section at 14 inches from the end is shown in the composite in **Figure 64** with the cross-

sections at 4 inches and 8 inches from the end. Cracking associated with the longest horizontal side crack remains visible in the cross-section surface at 14 inches from the end. This end of tie NDT #1 is another example of a tie with no visual top surface indications of distress that has developed a significant pattern of cracking along the sides and within the cross-section of the tie that is progressing towards upper surface delamination and tie failure.

The CXT identification markings on this tie include "505S", "357-D" and beneath the date plug "G1041" and "6" indicating 2006.

### DISCUSSION AND CONCLUSIONS

The findings of this investigation confirm that there is a general pattern to the onset and propagation of cracks in the prestressed concrete ties. Typically, cracking once initiated is present as horizontal cracks along the sides of the ties at slightly less than 50 percent of the tie height from the top surface. The pair of horizontal cracks generally penetrate to a location and depth inside the tie associated with the second row of prestressing wires from the top which have the outboard wires at closest proximity to the sides of the ties. With continued aging and service, cracking progresses further along the sides from the ends and further into the cross-section of the tie connecting the end wires in the second row from the top to the end and center wires in the top row. Continued cracking within the tie is exhibited as a pattern of cracks interconnecting wire location to wire location, generally around the outer perimeter wires and eventually progressing inward.

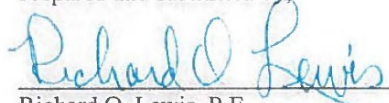
The depth of retreat of the wire ends that was recorded prior to sectioning and shown in **Appendix A** shows a general pattern of most significant retreat in the two top rows of wires and progressively less towards the bottom rows. That finding and observation is consistent with general pattern of crack progression along the sides and into the ties at the elevation of the second row of wires from the top. A greater extent of cracking damage in that location corresponds with the retreat of the wires in the same location and progressive loss of bond and prestress starting at the ends of the ties.

The pattern of progression of cracks based upon these findings does not include cracking visible in the top surface until the side and cross-section cracks have progressed to a moderate stage of deterioration. The top cracks are a later-in-time indication of onset of cracking and deterioration and unfortunately not an early indicator of the process. The ties documented in this investigation demonstrate that by the time a crack is visible in the top chamfer and top surface to

a length of several inches, the pattern of cracking along the sides of the tie and within the tie has progressed significantly.

Comparison of visual in-service indications of distress with the actual extent of cracking present and the impact echo findings indicates that the in-service top surface visual inspection is far less capable of identifying ties in the early stages of cracking and deterioration compared to the impact echo NDT methodology. Two of the ties sectioned and documented had no visual indications of cracking and a visual condition rating of "1" at one end but an NDT rating of either "2" or "3." Those examples were tie NDT #2 South End and NDT #1 South End. In both examples, horizontal cracking along the sides and within the cross-section between wires had progressed significantly yet there were no top surface indications of cracking. The results of this investigation demonstrate a viable correlation between the presence of cracking and detection by the impact echo response of the tie for tie conditions where the top surface visual indicators of cracking and distress are absent.

Prepared and submitted by,

  
Richard O. Lewis, P.E.

DECEMBER 4, 2012

APPENDIX A

DEPTH OF RETREAT OF WIRES AT THE ENDS OF THE TIES



DEPTH OF WIRE RETREAT AT END OF TIES (inch)			
WIRE NO.*	Tie NDT #7-S	Tie NDT #7-N	Tie NDT #69-N
1	0.043	0.044	0.052
2	0.038	0.051	0.068
3	0.035	0.054	0.071
4	0.038	0.078	0.061
5	0.039	0.034	0.057
6	0.026	0.035	0.047
7	0.028	0.038	0.046
8	0.043	0.080	0.050
9	0.032	0.025	0.047
10	0.027	0.029	0.040
11	0.028	0.034	0.036
12	0.037	0.038	0.031
13	0.035	0.015	0.040
14	0.025	0.027	0.038
15	0.026	0.025	0.030
16	0.023	0.038	0.021
17	0.022	0.011	0.038
18	0.018	0.019	0.033
19	0.019	0.018	0.036
20	0.023	0.028	0.020

\* Wire numbering convention facing the end of the tie, No.1 top row left side, ascending left to right and top row to bottom row.

DEPTH OF WIRE RETREAT AT END OF TIES (inch)			
WIRE NO.*	Tie NDT #1-S	Tie NDT #2-S	Tie NDT #2-N
1	0.082	0.100	0.148
2	0.108	0.089	Spalled
3	0.102	0.077	Spalled
4	0.091	0.064	Spalled
5	0.083	0.111	0.125
6	0.065	0.063	0.120
7	0.093	0.051	Spalled
8	0.140	0.065	Spalled
9	0.087	0.080	0.073
10	0.063	0.046	0.094
11	0.092	0.045	0.125
12	0.099	Spalled	0.151
13	0.076	Spalled	0.069
14	0.049	0.035	0.085
15	0.083	0.051	0.092
16	0.088	Spalled	0.094
17	Spalled	0.032	0.045
18	Spalled	0.046	0.072
19	0.075	0.027	0.061
20	0.072	Spalled	0.070

\* Wire numbering convention facing the end of the tie, No.1 top row left side, ascending left to right and top row to bottom row.

PRESTRESSED CONCRETE RAILROAD TIE INVESTIGATION



**Figure 1.** Side view of prestressed concrete railroad tie identified as NDT #7, manufactured by CXT at Grand Isle, Nebraska in 2006. L3672 102312 01



**Figure 2.** Tie NDT #7 with the NDT transducer array positioned on the top of the tie as employed in the impact echo testing. L3672 102312 16

*Lewis Engineering and Consulting, Inc.*

PRESTRESSED CONCRETE RAILROAD TIE INVESTIGATION



**Figure 3.** Closer view at the south end of tie NDT #7 showing distance from most outboard transducer to the end of the tie during testing. L3672 102312 17

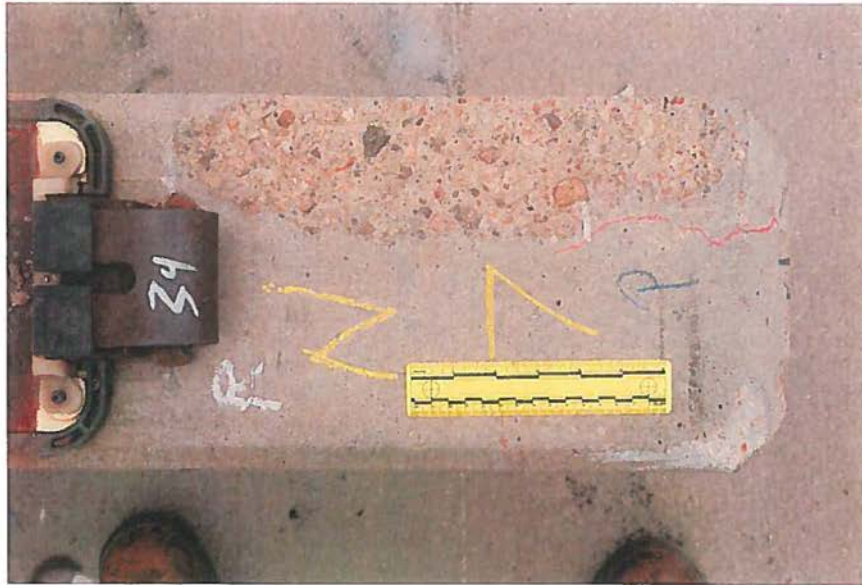


**Figure 4.** Top surface at north end of the NDT #7 rated by NDT as condition "5". L3672 102312 02

*Lewis Engineering and Consulting, Inc.*

PRESTRESSED CONCRETE RAILROAD TIE INVESTIGATION

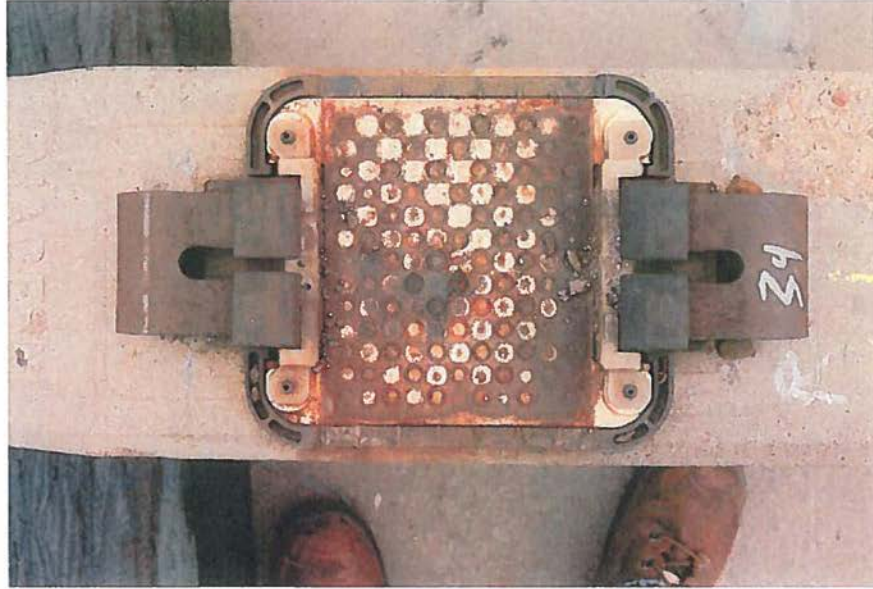
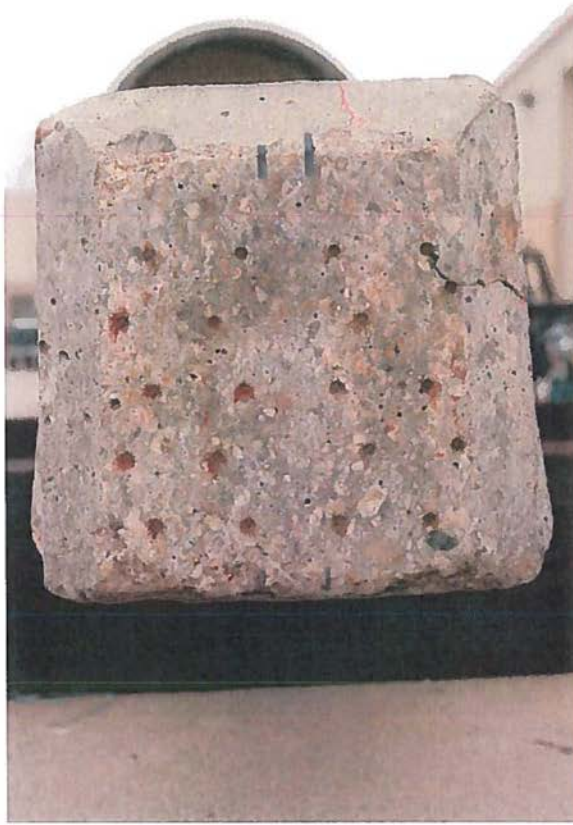


Figure 5. North end track pad on tie NDT #7. L3672 102312 03



PRESTRESSED CONCRETE RAILROAD TIE INVESTIGATION



**Figure 6.** North end view of tie NDT #7 with retreated wire ends and visible crack at right. L3672 102312 04

*Lewis Engineering and Consulting, Inc.*



PRESTRESSED CONCRETE RAILROAD TIE INVESTIGATION



Figure 7. Side view of north end of the NDT #7, visible crack outlined in red.

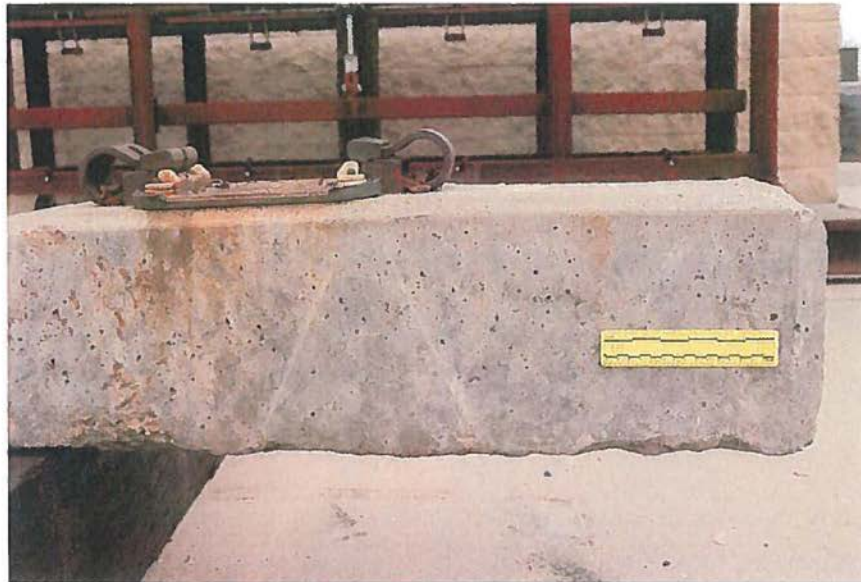
L3672 102312 05



Figure 8. Closer side view at north end of tie NDT #7. L3672 102312 06

*Lewis Engineering and Consulting, Inc.*

PRESTRESSED CONCRETE RAILROAD TIE INVESTIGATION



**Figure 9.** Opposite side view at north end of tie NDT #7, visible crack not outlined in red. L3672 102312 07



**Figure 10.** Close side view at north end of tie NDT #7, visible crack not outlined. L3672 102312 08

*Lewis Engineering and Consulting, Inc.*



PRESTRESSED CONCRETE RAILROAD TIE INVESTIGATION

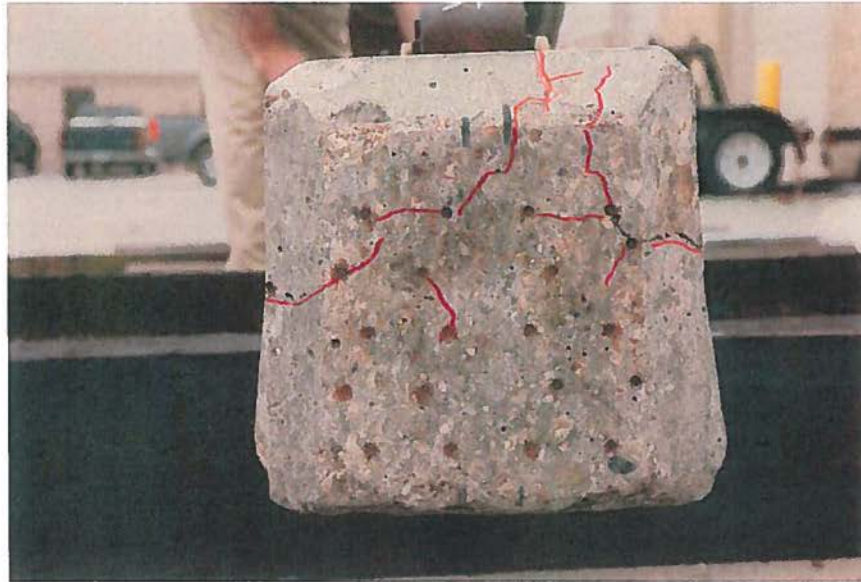


**Figure 11.** North end view of tie NDT #7 with visible cracks outlined in red.

L3672 102312 22

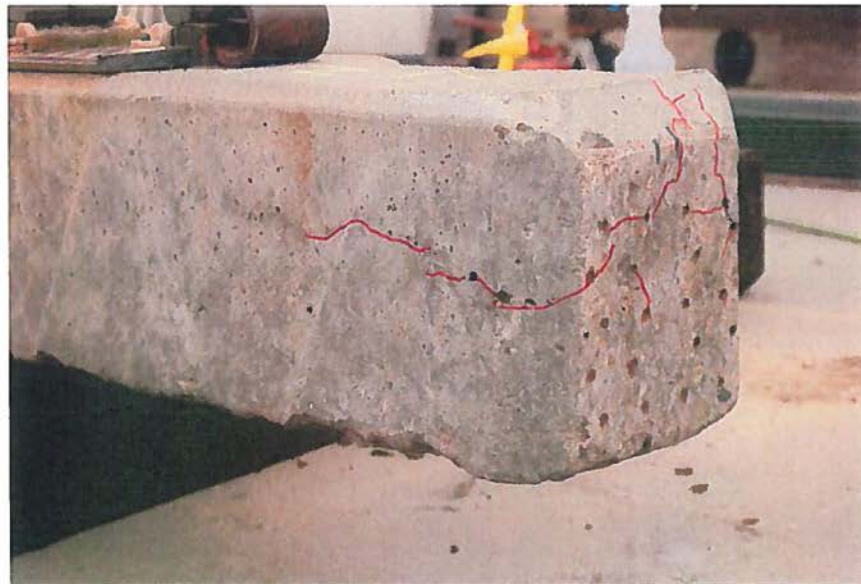


**Figure 12.** Oblique view of one side and north end of NDT #7 with all visible cracks outlined; side crack extends 8 inches from end. L3672 102312 23

*Lewis Engineering and Consulting, Inc.*

PRESTRESSED CONCRETE RAILROAD TIE INVESTIGATION

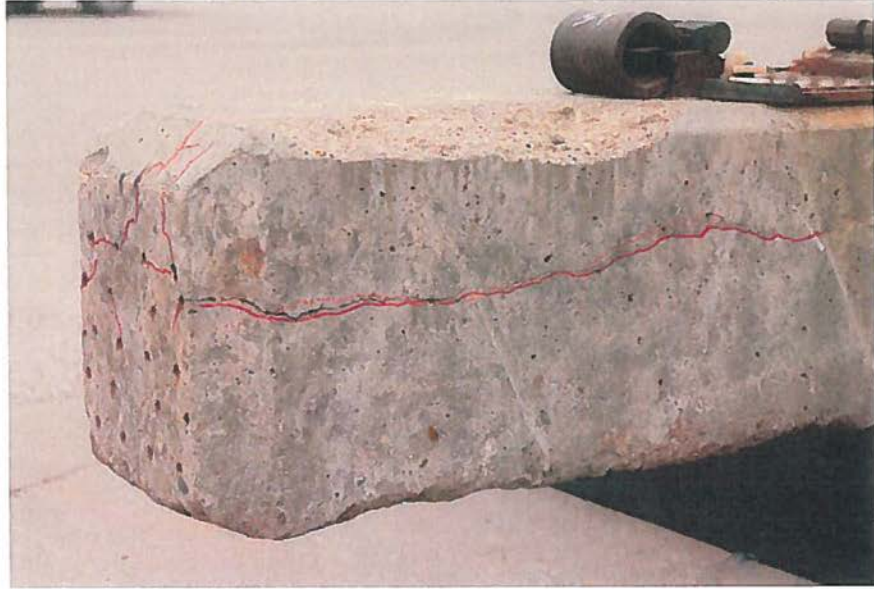


**Figure 13.** Oblique view showing north end and opposite side of tie with visible cracks outlined; side crack extends 15 inches from end. L.3672 102312.23

PRESTRESSED CONCRETE RAILROAD TIE INVESTIGATION



**Figure 14.** Cross-sections at saw cut locations on tie NDT #7 at 4 inches (left), 14 inches (center) and 21 inches (right) at center of rail pad, all visible cracks outlined in red.

*Lewis Engineering and Consulting, Inc.*

PRESTRESSED CONCRETE RAILROAD TIE INVESTIGATION



Figure 15. Top surface at south end of tie NDT #7 rated by NDT as "1" condition.  
L3672 102312 09

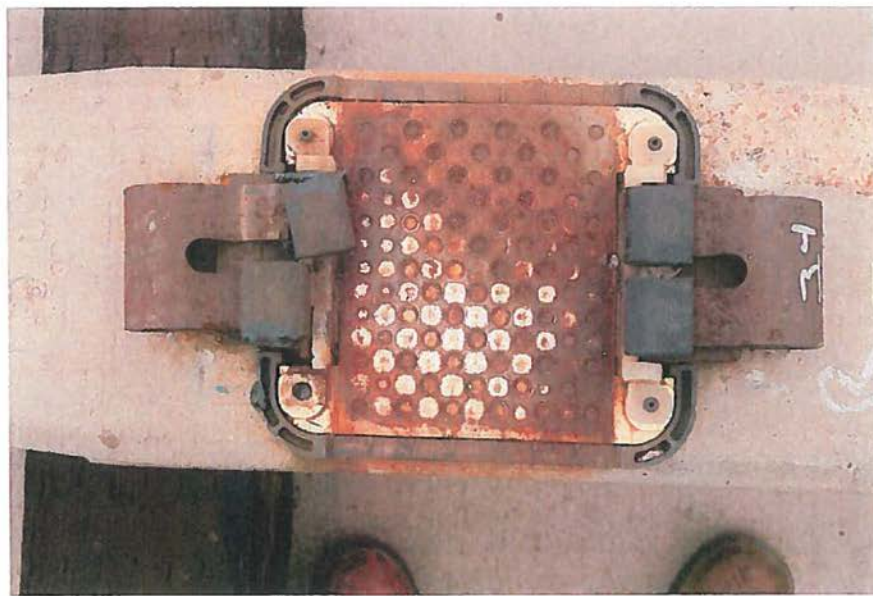


Figure 16. South end track pad on tie NDT #7. L3672 102312 10

*Lewis Engineering and Consulting, Inc.*



PRESTRESSED CONCRETE RAILROAD TIE INVESTIGATION



**Figure 17.** South end of tie NDT #7 without outlining of cracks. L3672 102312 11



**Figure 18.** Side view at south end of tie NDT #7. L3672 102312 12

*Lewis Engineering and Consulting, Inc.*

PRESTRESSED CONCRETE RAILROAD TIE INVESTIGATION

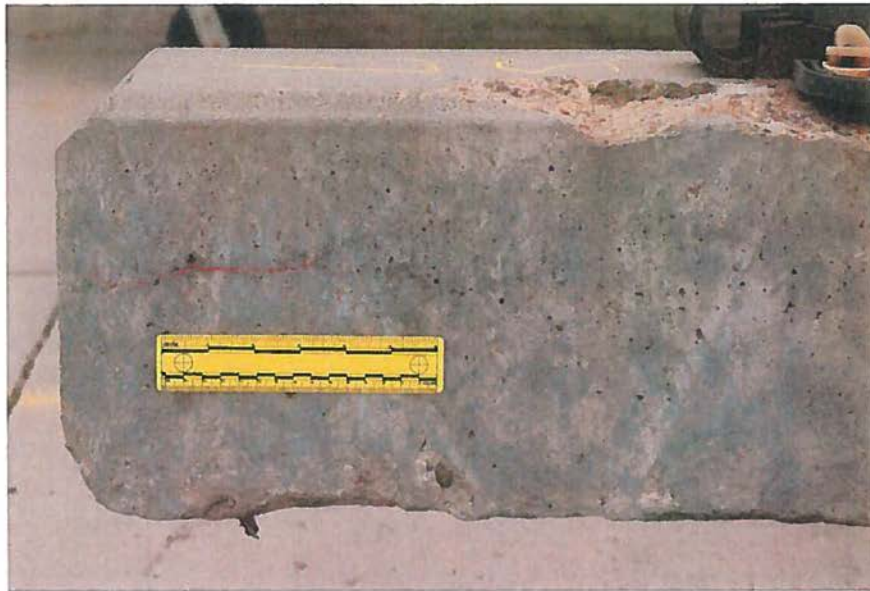


**Figure 19.** Closer view of side of tie NDT #7 at south end, outlined crack extends 6 inches from end. L3672 102312 13



**Figure 20.** Opposite side of south end of tie NDT #7. L3672 102312 14

*Lewis Engineering and Consulting, Inc.*

PRESTRESSED CONCRETE RAILROAD TIE INVESTIGATION

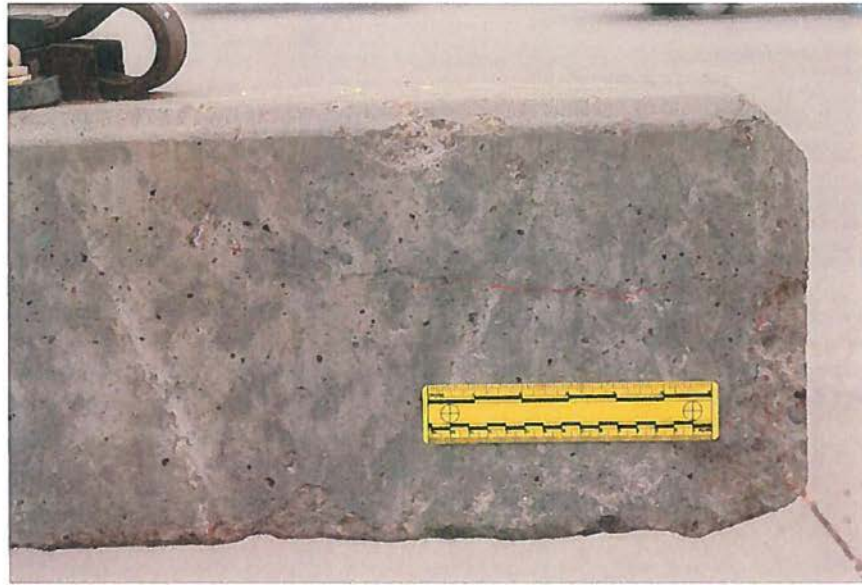


**Figure 21.** Closer view of opposite side of tie NDT #7 at south end, outlined crack extends 9 inches from end. L3672 102312 15



**Figure 22.** Oblique view of sections removed at 4 inches and 8 inches from south end of tie NDT #7 with cracks outlined in red. L3672 102312 19

*Lewis Engineering and Consulting, Inc.*



PRESTRESSED CONCRETE RAILROAD TIE INVESTIGATION



**Figure 23.** Opposite side view of two sections removed at 4 inches and 8 inches from south end of tie NDT #7. L3672 102312 20

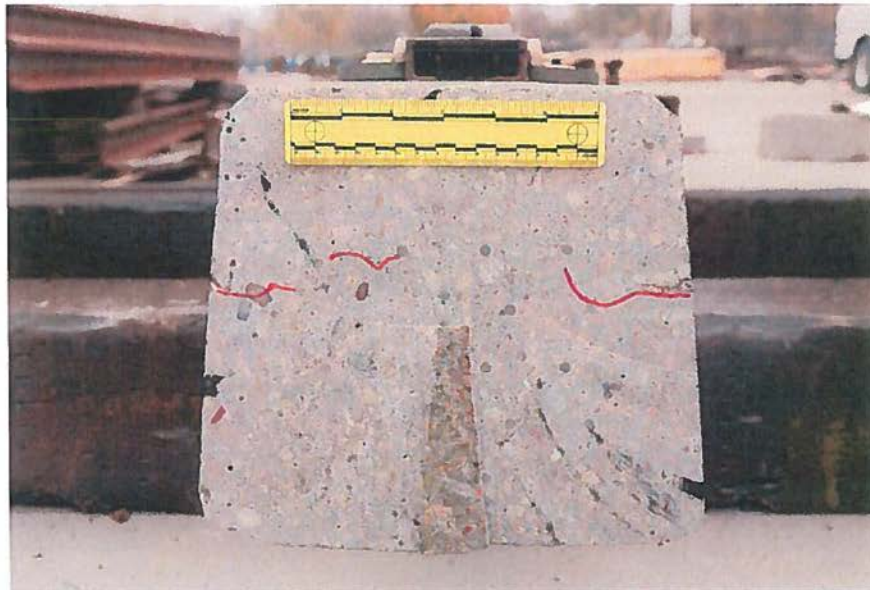


**Figure 24.** Cross-section of south end of tie NDT #7 at 4 inches from end with cracks outlined in red. L3672 102312 18

*Lewis Engineering and Consulting, Inc.*

PRESTRESSED CONCRETE RAILROAD TIE INVESTIGATION

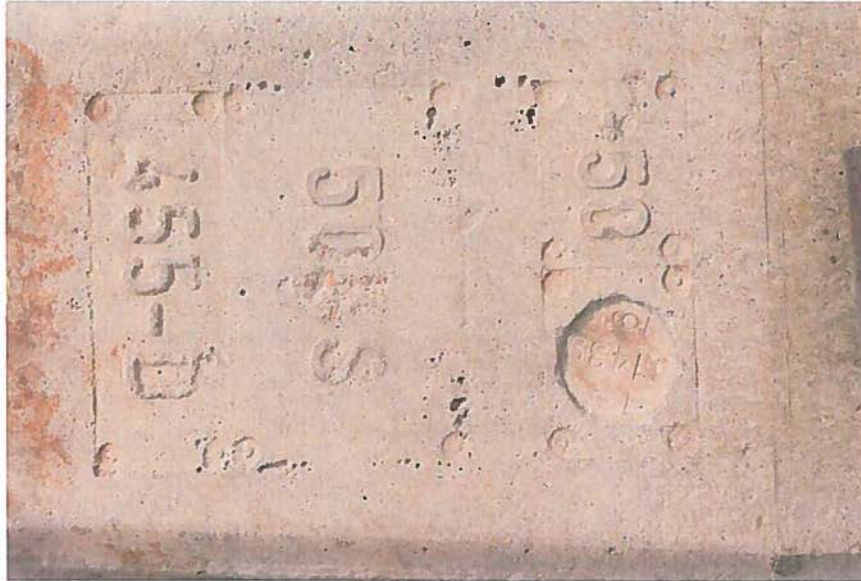


**Figure 25.** Cast identification information in tie NDT #7, beneath date plug reads G1439 and 6 for 2006. L.3672 102312 29



**Figure 26.** Tie NDT #69 with transducer array placed as employed in making impact echo recordings, rated by NDT as condition "2" both ends. L.3672 102312 30

*Lewis Engineering and Consulting, Inc.*

PRESTRESSED CONCRETE RAILROAD TIE INVESTIGATION

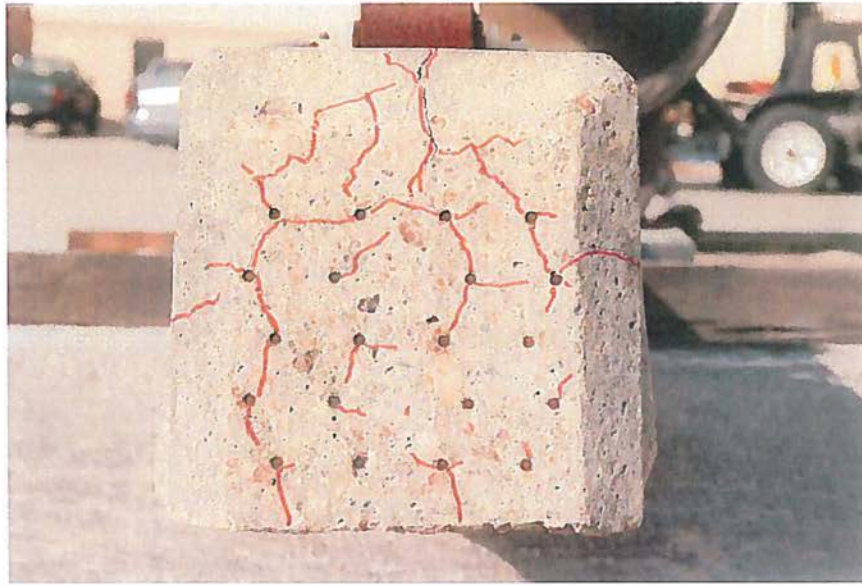


**Figure 27.** North end of tie NDT #69 with visible cracks outlined in red. L3672 102312 32

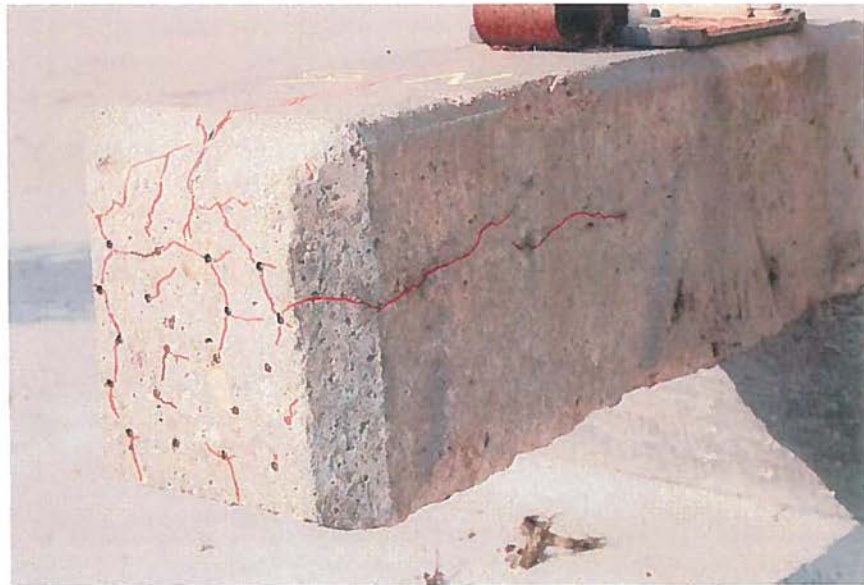


**Figure 28.** Oblique end view of north end of tie NDT #69 showing cracks also outlined on top and along one side. L3672 102312 33

*Lewis Engineering and Consulting, Inc.*



PRESTRESSED CONCRETE RAILROAD TIE INVESTIGATION



Figure 29. Opposite side oblique north end view of tie NDT #69. L3672 102312 34

PRESTRESSED CONCRETE RAILROAD TIE INVESTIGATION



**Figure 30.** North end cross-sections of tie NDT #69 at exposed end (left), saw cut at 4 inches (center) and saw cut at 8 inches (right), all visible cracks outlined in red.

*Lewis Engineering and Consulting, Inc.*

PRESTRESSED CONCRETE RAILROAD TIE INVESTIGATION

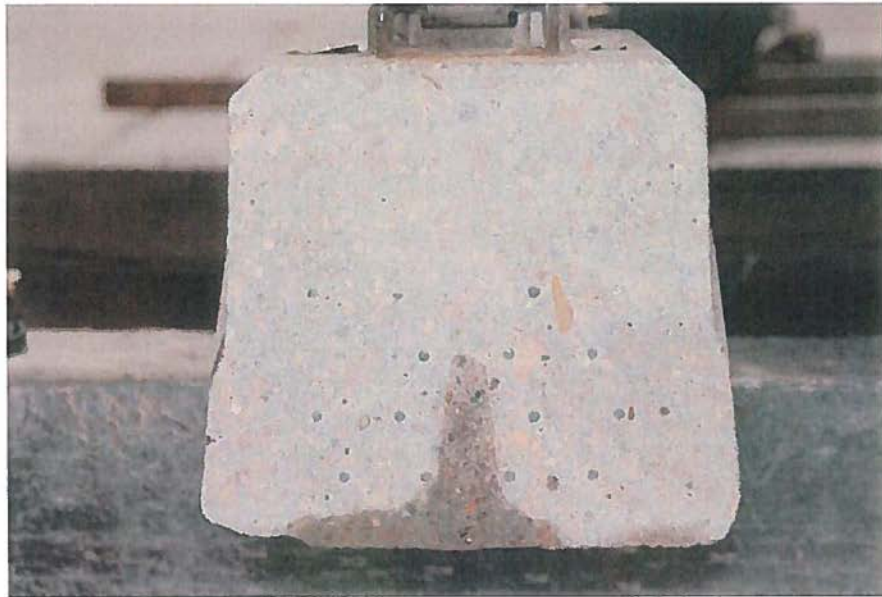


**Figure 31.** Cross-section of tie NDT #69 at saw cut 14 inches from end, no visible cracks. L3672 102312 44



**Figure 32.** Side view of successive sections removed at north end of tie NDT #69. L3672 102312 41

*Lewis Engineering and Consulting, Inc.*

PRESTRESSED CONCRETE RAILROAD TIE INVESTIGATION



Figure 33. Opposite side oblique view of successive sections removed at north end of tie NDT #69. L3672 102312 43

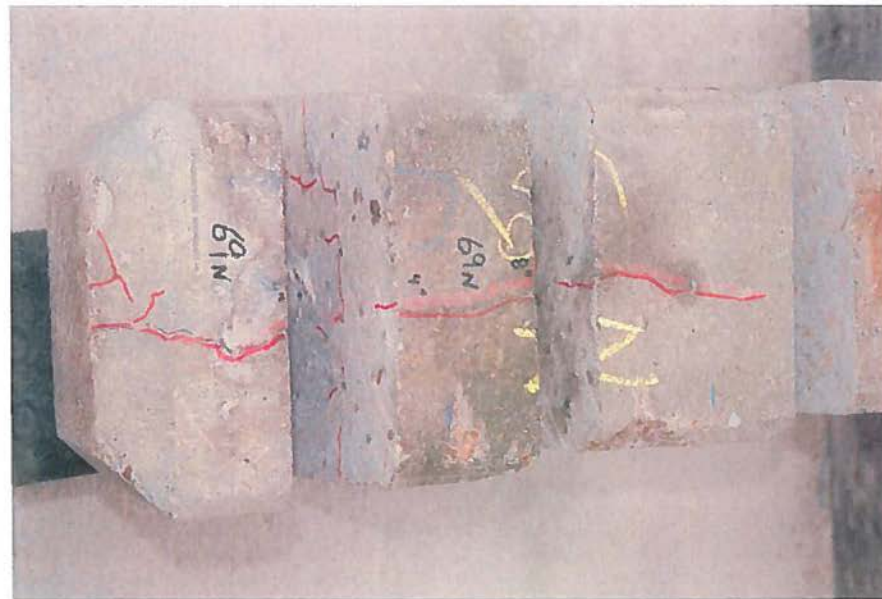


Figure 34. Top surface view of successive sections removed at north end of tie NDT #69. L3672 102312 42

Lewis Engineering and Consulting, Inc.



PRESTRESSED CONCRETE RAILROAD TIE INVESTIGATION

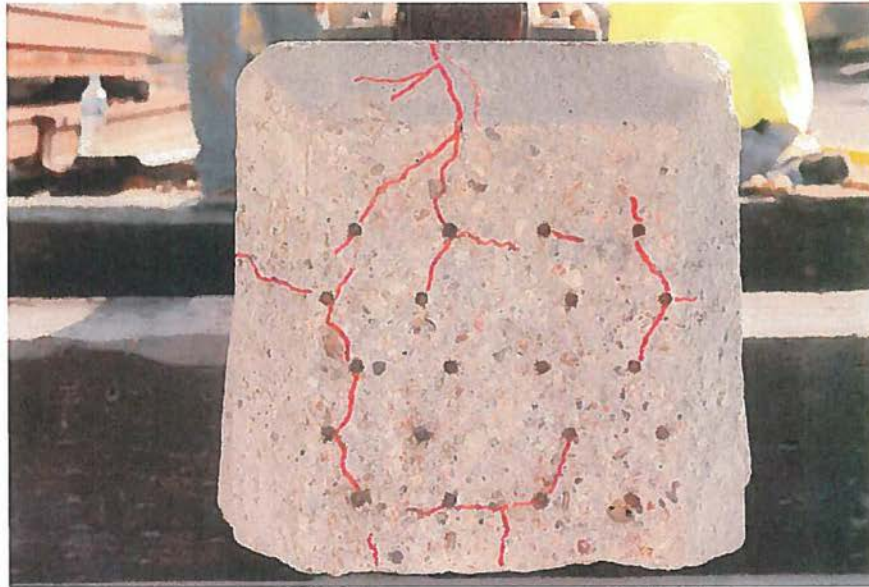


Figure 35. South end of tie NDT #69 showing visible cracks outlined in red, rated by NDT as condition "2". L3672 102312 35

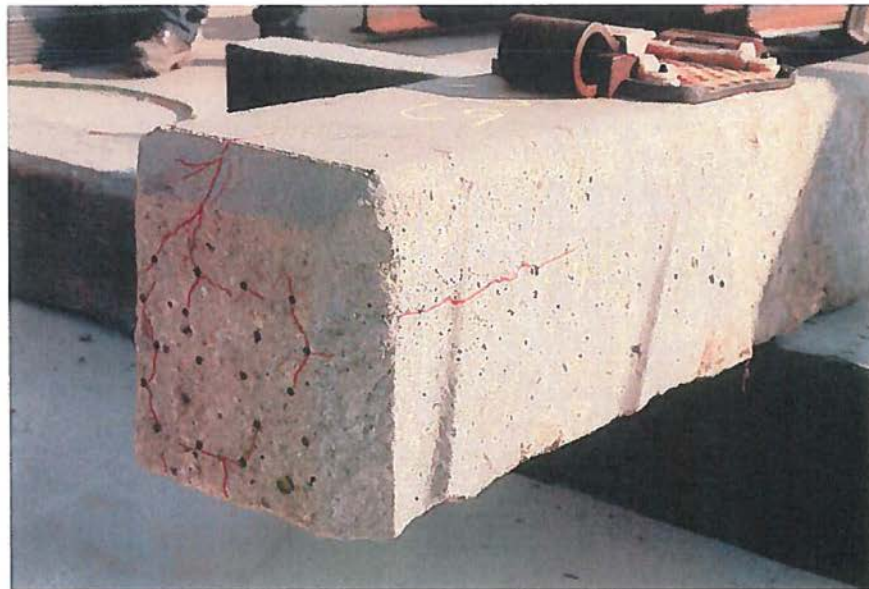


Figure 36. Oblique view of south end of tie NDT #69 with cracks outlined in red. L3672 102312 36

*Lewis Engineering and Consulting, Inc.*

7.

PRESTRESSED CONCRETE RAILROAD TIE INVESTIGATION



Figure 37. Opposite side oblique end view at south end of tie NDT #69. L3672 102312 37

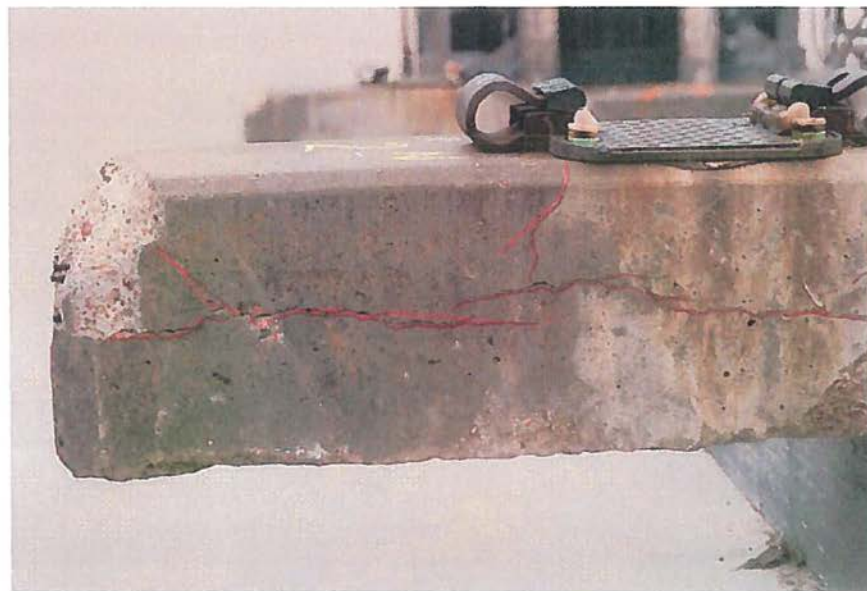
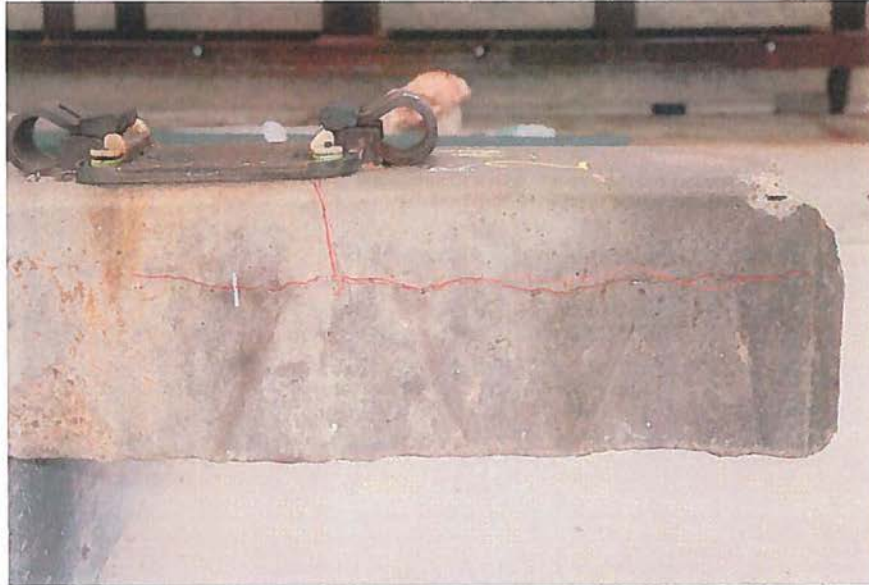


Figure 38. Side view of north end of tie NDT #2, rated by NDT as condition "4".  
L3672 102312 47

*Lewis Engineering and Consulting, Inc.*



PRESTRESSED CONCRETE RAILROAD TIE INVESTIGATION



**Figure 39.** Opposite side view of north end of tie NDT #2. L3672 102312 47



**Figure 40.** North end view of tie NDT #2, significant spalling at top chamfer.  
L3672 102312 48

*Lewis Engineering and Consulting, Inc.*

PRESTRESSED CONCRETE RAILROAD TIE INVESTIGATION



Figure 41. Top surface of north end of tie NDT #2. L3672 102312 46

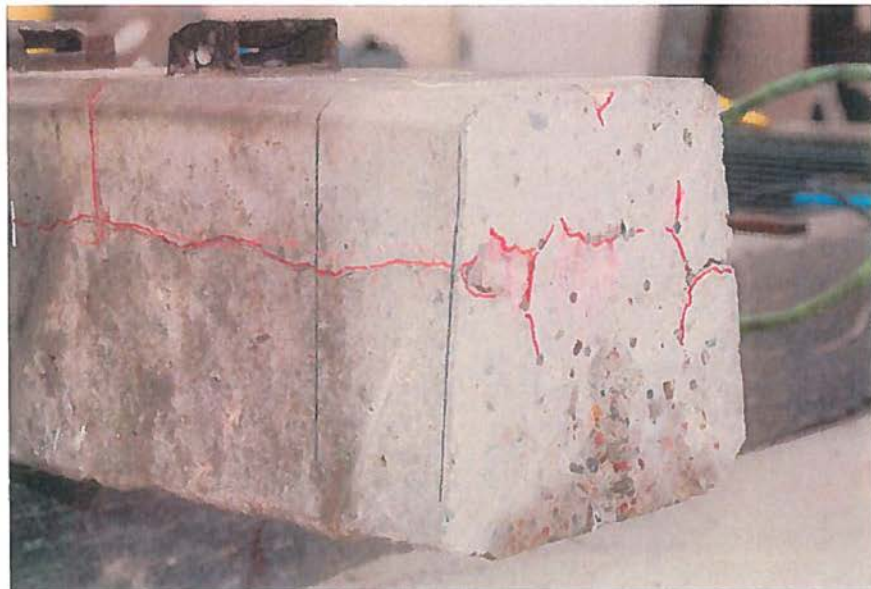
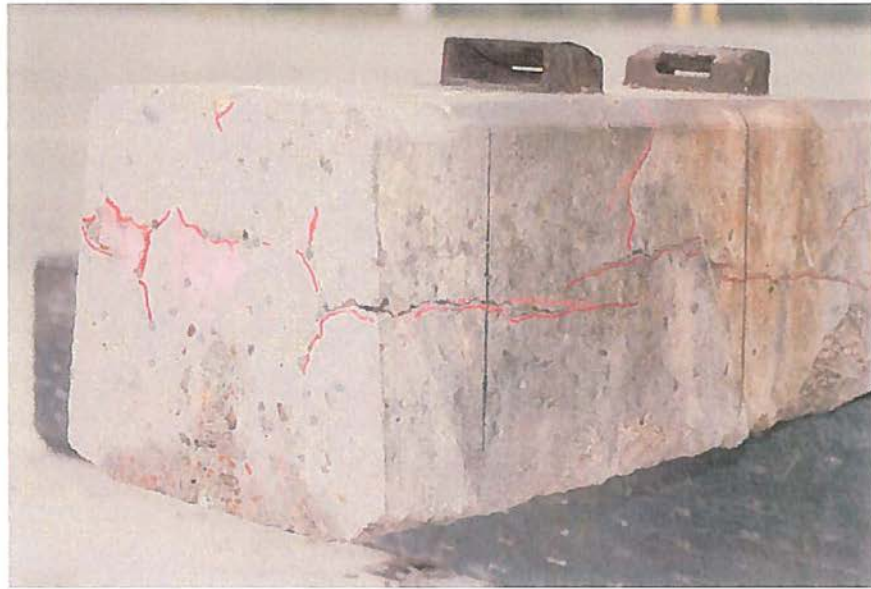


Figure 42. Oblique side view of tie NDT #2 after removal of 6 inches at end.

L3672 102312 50

*Lewis Engineering and Consulting, Inc.*

PRESTRESSED CONCRETE RAILROAD TIE INVESTIGATION



**Figure 43.** Opposite side oblique end view of tie NDT #2 after removal of 6 inches at end. L3672 102312 51



**Figure 44.** Oblique side view of tie NDT #2 after removal of 10 inches at end.

L36372 102312 54

*Lewis Engineering and Consulting, Inc.*



PRESTRESSED CONCRETE RAILROAD TIE INVESTIGATION



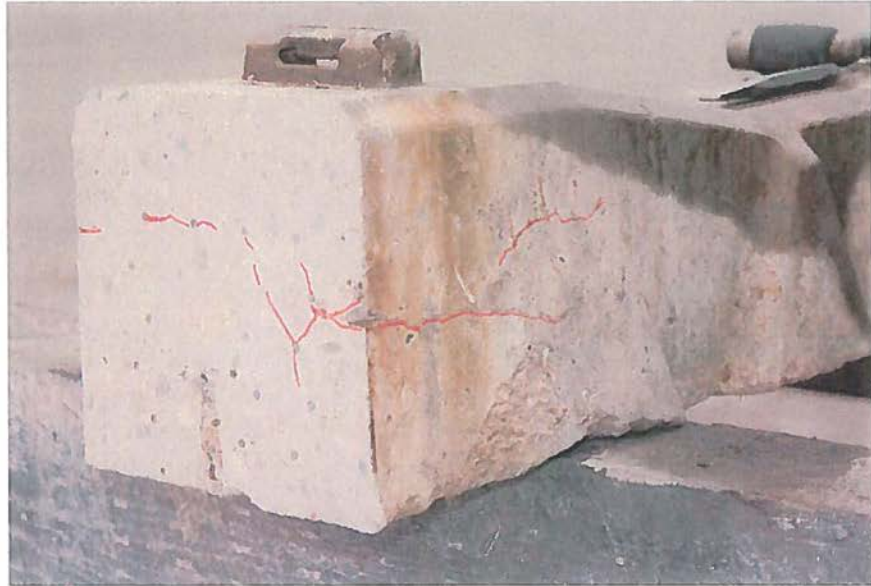
Figure 45. Opposite side oblique end view of tie NDT #2 after removal of 10 inches at end. L3672 102312 52



Figure 46. Oblique side view of tie NDT #2 after removal of 21 inches at end, center of rail pad. L3672 102312 58

*Lewis Engineering and Consulting, Inc.*

PRESTRESSED CONCRETE RAILROAD TIE INVESTIGATION



**Figure 47.** Opposite side oblique view of tie NDT #2 after removal of 21 inches at end. L3672 102312 57



PRESTRESSED CONCRETE RAILROAD TIE INVESTIGATION



**Figure 48.** North end cross-sections of tie NDT #2 at saw cuts at 6 inches (left), 10 inches (center) and 21 inches at center of rail pad (right), all visible cracks outlined in red.

PRESTRESSED CONCRETE RAILROAD TIE INVESTIGATION



**Figure 49.** Cross-section at saw cut 28 ½ inches from north end of tie NDT #2, inboard of rail pad towers. L3672 102312 60

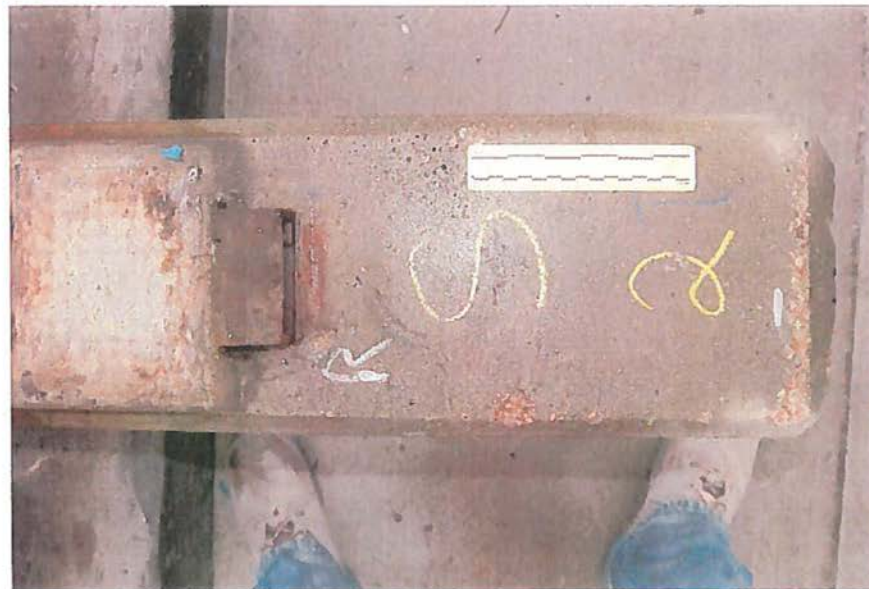


**Figure 50.** Top view of south end of tie NDT #2 rated by NDT as condition "2". L3672 102312 61

*Lewis Engineering and Consulting, Inc.*

PRESTRESSED CONCRETE RAILROAD TIE INVESTIGATION

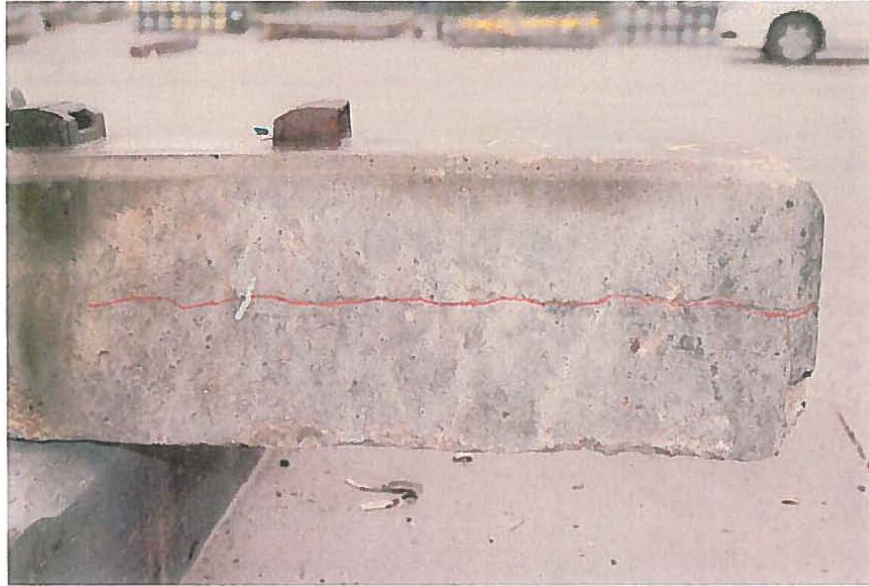


**Figure 51.** Side view of south end of tie NDT #2, horizontal crack outlined in red.

L3672 102312 62



**Figure 52.** Opposite side view of south end of tie NDT #2. L3672 102312 63

*Lewis Engineering and Consulting, Inc.*

PRESTRESSED CONCRETE RAILROAD TIE INVESTIGATION



**Figure 53.** South end of tie NDT #2, cracks outlined in red. 1.3672 102312 64

PRESTRESSED CONCRETE RAILROAD TIE INVESTIGATION

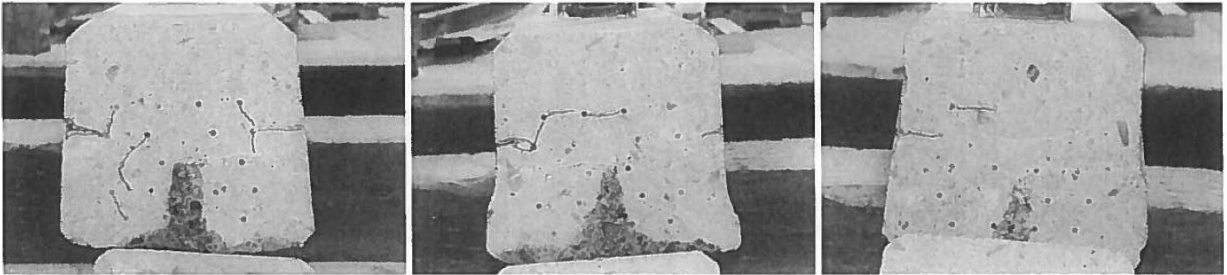


Figure 54. South end cross-sections of tie NDT #2 at saw cuts 4 inches (left), 8 inches (center) and 14 inches (right) from end, cracks outlined in red.

*Lewis Engineering and Consulting, Inc.*





Figure 55. Overall view of tie NDT #1 rated by NDT as condition "2" on north end, and condition "3" on south end. L3672 102512 71



Figure 56. Top surface of south end of tie NDT #1 rated condition "3" by NDT and condition "1" by visual. L3672 102512 73

**FRESTRESSED CONCRETE RAILROAD TIE INVESTIGATION**



**Figure 57.** Side view of south end of tie NDT #1 with horizontal crack 21 inches long outlined in red. L3672 102512 74



**Figure 58.** Opposite side view of south end of tie NDT #1 with horizontal crack 13 inches long outlined in red. L3672 102512 75

PRESTRESSED CONCRETE RAILROAD TIE INVESTIGATION

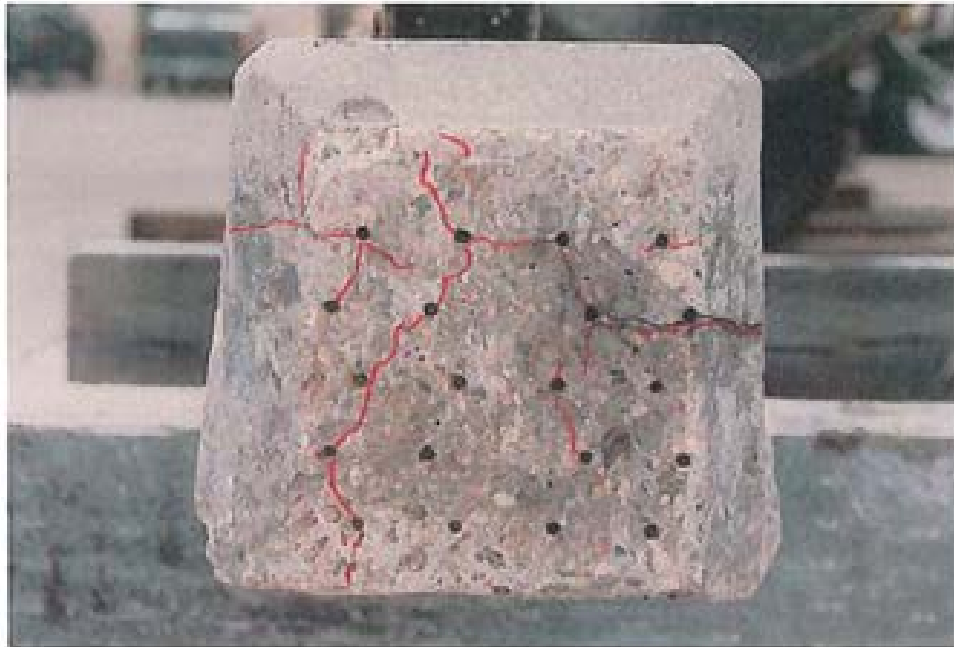


Figure 59. South end of tie NDT #1 with cracks outlined in red. L3472 102312 74



Figure 60. Oblique view of south end of tie NDT #1 after removal of 4 inches, cracks outlined in red. L3472 102312 77

PRESTRESSED CONCRETE RAILROAD TIE INVESTIGATION



Figure 61. Opposite side oblique view of south end of tie NDT #1 after removal of 4 inches. L3672 103312 80



Figure 62. Oblique view of south end of tie NDT #1 after removal of 8 inches from end. L3672 103312 84

*Lewis Engineering and Consulting, Inc.*

PRESTRESSED CONCRETE RAILROAD TIE INVESTIGATION

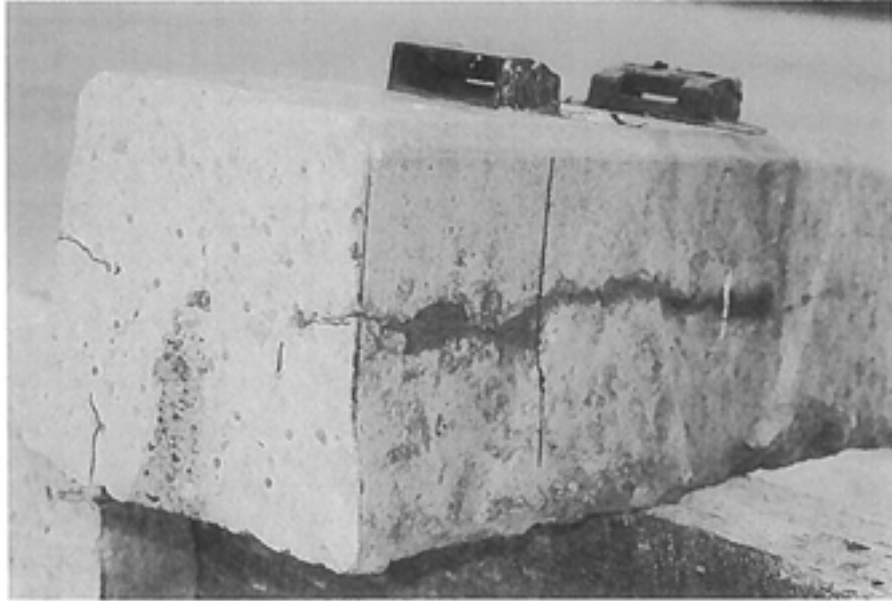


Figure 63. Opposite side oblique view of south end of tie NDT #1 after removal of 8 inches from end. L3672 102312 83



PRESTRESSED CONCRETE RAILROAD TIE INVESTIGATION

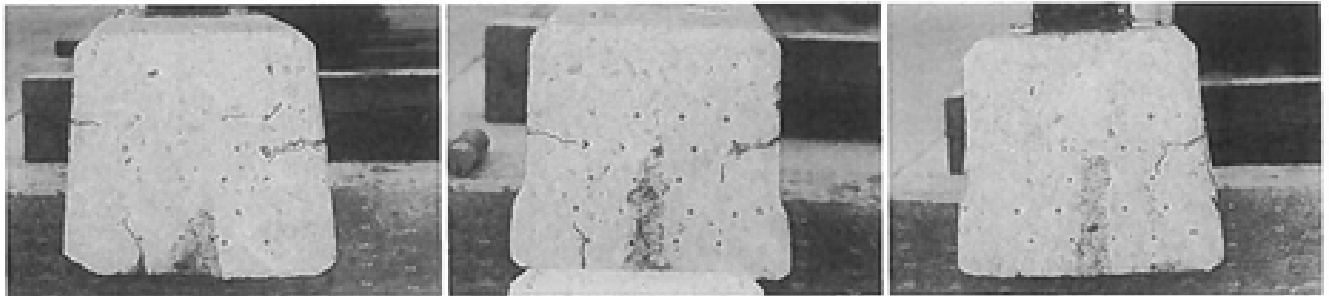


Figure 6-4. South end cross-sections of tie NDT #1 at saw cuts 4 inches (left), 8 inches (center) and 14 inches (right) from end, cracks outlined in red.

*Lewis Engineering and Consulting, Inc.*

**APPENDIX 2**  
**SONIC/ULTRASONIC MEASUREMENTS**

## APPENDIX SONIC/ULTRASONIC NONDESTRUCTIVE TESTING OF CONCRETE

The sonic/ultrasonic measurements made to determine the characteristics of concrete (or rock) are generated by a relatively low energy source as a single discrete wide band impulse with a pulsed transducer, projectile, mechanical hammer, etc. Practical problems and the condition of the concrete surface largely determine the source(s) to be used. A rough concrete surface that has deposits of organic materials or mineral deposits generally requires a more powerful energy source whereas a relatively new or wet concrete may be inspected by the use of a pulsed transducer or other higher frequency source. In general high frequency sources that may work well in the laboratory may be unusable for field conditions. High frequency sources have the advantage of high resolution but the disadvantage of low penetration. While metals can be tested in the megahertz range, such signals in concrete will not have measurable signals for more than an inch in thickness. The energy source should be sufficient to maximize the resolution, have sufficient penetration to examine the concrete being tested and enough energy to excite the fundamental frequencies being sought.

The transmitted energy is in the form of three principal wave types: compressional (contraction/expansion, spring-like particle motion), shear (traction-sliding motion), and surface waves (combination of motions). Each boundary that has density and or velocity contrast will reflect and/or refract these waves. Compressional and shear wave velocity values are determined by the Young's, shear and bulk moduli values as well as the density and Poisson's Ratio. In turn the velocity can be used to determine the moduli values and Poisson's Ratio given that the density is known or can be assumed. The moduli values measured are the dynamic moduli values at low strain. In general, the difference between the dynamic values and the static values is almost entirely controlled by the crack densities of the concrete. Using the modulus values, a reasonable estimate of the unconfined compressive strength can be determined. The strength is largely dependent on the crack density of the concrete and for static tests, the orientation of the cracks. For static testing, cracks perpendicular to the axis of the core and perpendicular to the directed stress will produce a strength (static) that is not greatly different from uncracked concrete. The applied stress closes or compresses the cracks. Cracks that are near 45° to the direction of stress will result in lowest static strength. The approximate orientation of the cracks can be determined with dynamic measurements of the velocity values in different directions.

NDT Corporation makes several determinations from one energy impact. The velocity is measured directly from the energy point of impact to a linear array(s) of sensors on the surface. The array length is usually in excess of the thickness of the concrete being tested. In addition to the velocity measurements, reflections are measured individually or determined from a frequency analysis of the time domain recordings. Each reflecting surface (change of density and/or velocity) produces a multi-path reflection in the layer it bounds. A generated wave will travel to a delamination surface and reflect back to the surface of the concrete where it is reflected back to the delamination, resulting in multi-reflections that are apparent in the frequency domain. These reverberations (echoes) are particularly diagnostic of delaminations and thickness of the concrete. They will readily distinguish the presence of local delaminations, cracked or decomposed inclusions by the particular frequency band generated at the mechanical discontinuity. If a delamination is

$$\frac{D}{T} = \frac{D - 2 \tan \Theta}{V_2} + \frac{2T}{V_1 \cos \Theta}$$

The thickness is expressed as:

$$T = \frac{D_{\text{@}}}{2} \sqrt{\frac{V_2 - V_1}{V_2 + V_1}}$$

$D$  is the distance and  $T$  is the thickness. Since the times as well as the distances are measured, then  $V_1$  and  $V_2$  are determined. If a plot of distance versus time is made then the resulting graph will look like Figure A2.

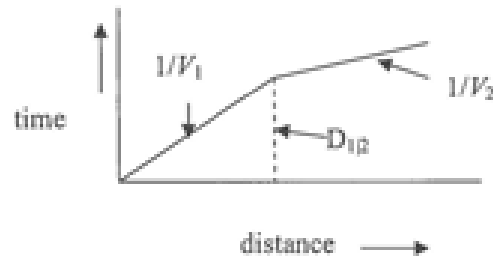


Figure A2

If the concrete has no overlay then the concrete velocity is simply  $D/T$ .

The resonant frequencies are determined by the thickness and velocity of the material. Since the velocity is measured as above, then the thickness can be determined directly.

The resonance of a simple beam is given by:

$$f = \frac{nV}{2L} \quad (\text{fixed - fixed, free - free}) \quad \text{where } n = 1, 2, 3, \dots$$

$$f = \frac{nV}{4L} \quad (\text{open - fixed}), \quad \text{where } n = 1, 3, 5, 7, \dots$$

Since the frequency and velocity are measured, the thickness is determined. This thickness can be the thickness of the concrete floor, deck slabs, or column being measured or it can be the thickness of concrete overlying a delamination.

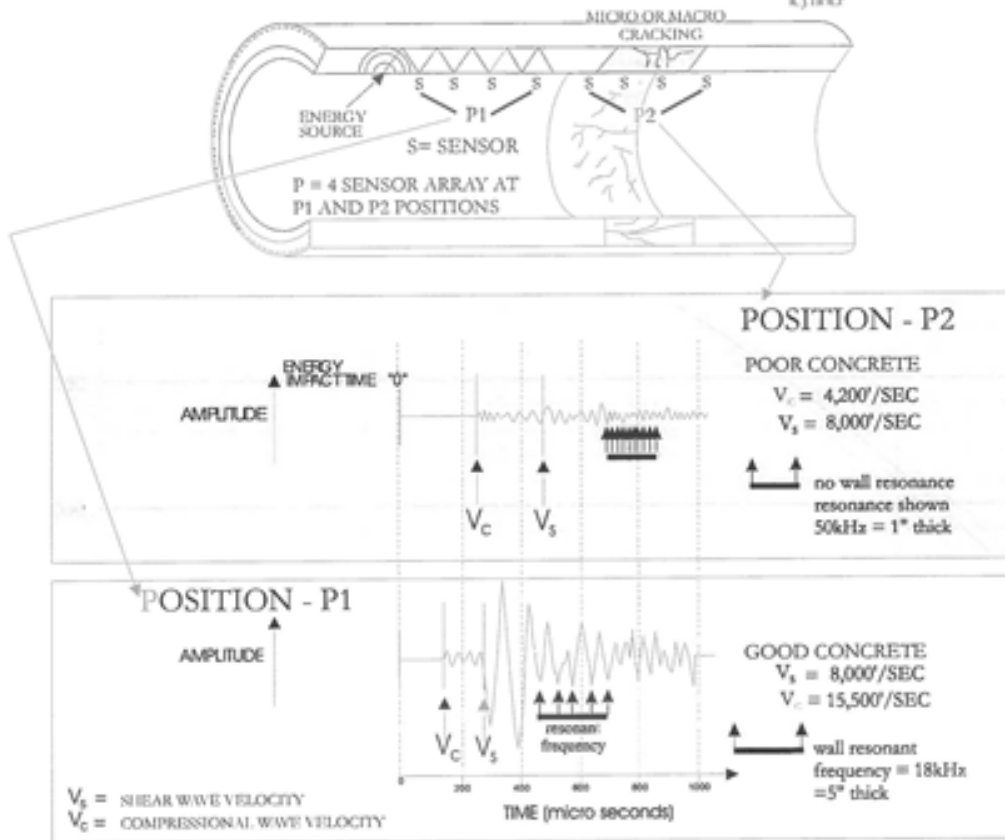
While the refracted wave is dependent only on a contrast in velocity, a reflection can take place where there is a change in velocity or density or both. The impedance (RF reflection coefficient) which causes a wave to be reflected is given by:

# SONIC/ULTRASONIC TUNNEL & PIPE LINE TESTING

Circumferential (face to back) Cracking

NDT ENGINEERING, INC.

8, J 1987



SONIC/ULTRASONIC TIME AMPLITUDE RECORDS FOR FOURTH SENSOR - POOR AND GOOD CONCRETE

FIGURE A3



SHEAR MODULUS - SHEAR VELOCITY

NDT ENGINEERING, INC.  
R.J.HOLT

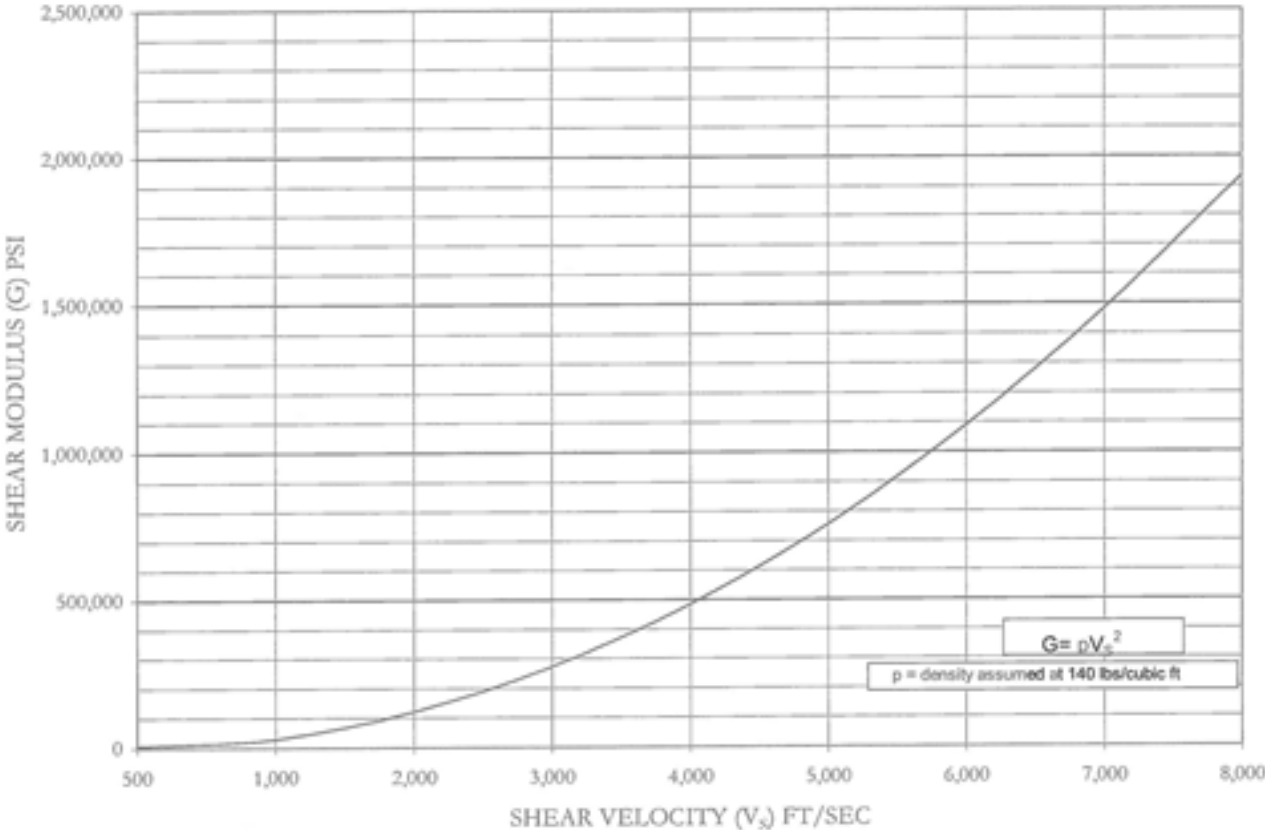
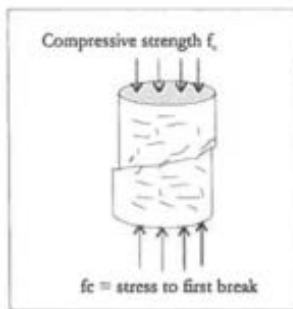
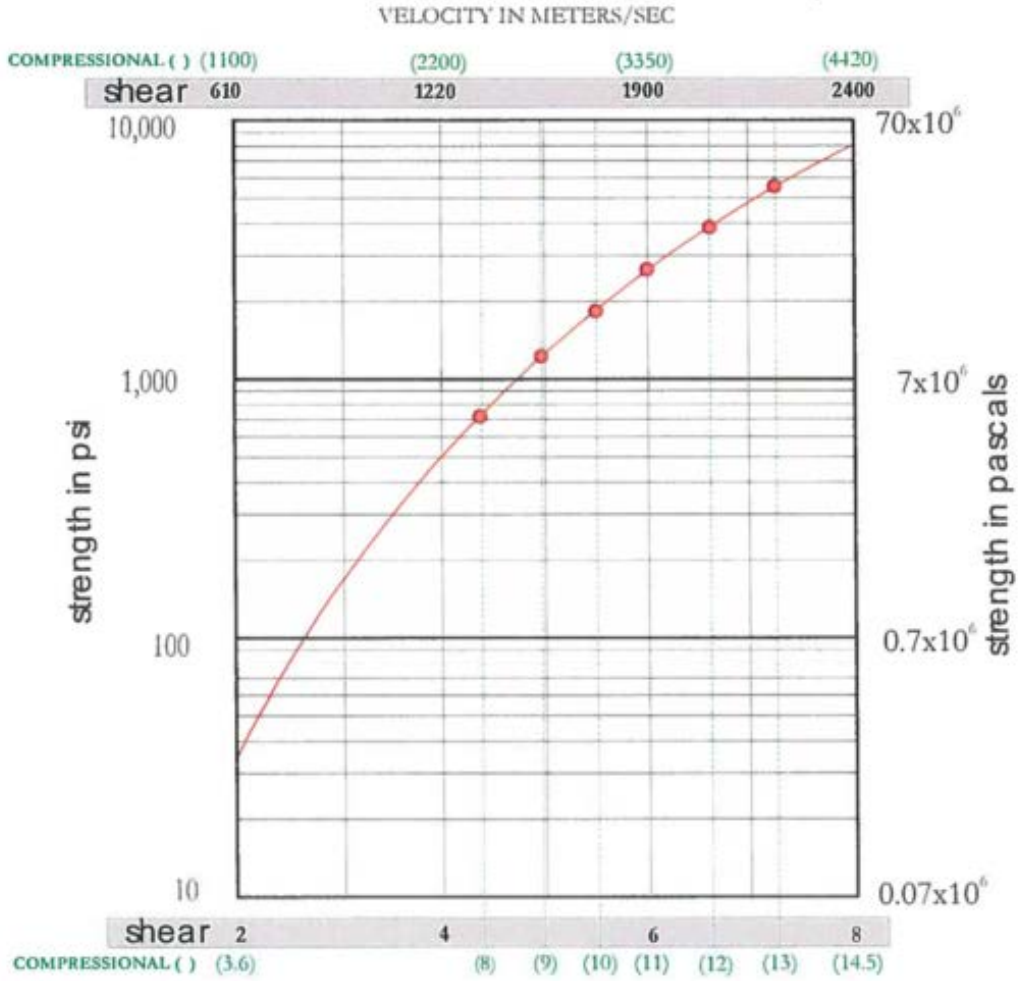


Figure A5

# strength of concrete versus velocity

r. j. holt



VELOCITY IN FEET/SEC (X 1,000)

CURVE FOR RATIO:  $V_{SHEAR} / V_{COMPRESSIONAL} = 0.55$   
 EQUALS POISSON'S RATIO OF 0.28

FIGURE A7  
 NDTENGINEERING, INC.

# **SONIC/ULTRASONIC TESTING OF METRO-NORTH CONCRETE CROSSTIES**



**BY  
NDT CORPORATION**

**March 2013**

## **Summary of Results:**

NDT Corporation conducted sonic/ultrasonic impact velocity and echo nondestructive testing of 60 pre-stressed concrete railroad crossties on Track 1 North of the Fordham Station in the Bronx New York (Figure 1). The objective of this testing was to: 1) evaluate the performance of NDT Corporation's Automated Crosstie Testing Device; 2) to obtain data on an active line to determine what effect (if any) ballast, communication signals and rails have on impact velocity and echo data and 3) determine rate ties tested.

### **Automated Device Performance:**

- Mechanical changes to the sensor rotation drive have eliminated sensor dragging across the top of the tie and resulted in the system acquiring high quality data at production speeds.
- System is able to acquire quality impact velocity and echo data at a rate of 1 tie per second.
- Transport Projectile guns separate and install when on the rail so they do not get damaged in transit.

### **Data Quality:**

- Data quality was similar to data acquired in yard test with hand held device. Resonant frequencies were a little noisier but tie thickness resonances were evident.
- Resonant frequencies and compressional and shear wave velocity values used to evaluate tie conditions were present on all four sensors for most ties.

### **Tie Condition Rating:**

- All sixty (60) of the ties tested during this testing program have data that indicate there is little to no internal cracking.

## **Introduction:**

NDT Corporation with the assistance of Metro-North conducted nondestructive sonic/ultrasonic measurements on sixty concrete railroad crossties on Track-1 north of the Fordham Station (Figure 1) on March 21, 2013. All of the ties tested during this investigation were manufactured by KSA.

### **Sonic/ultrasonic Nondestructive Testing Measurements:**

Sonic/ultrasonic measurements determine the mechanical characteristics of concrete as determined by their direct sonic compressional and shear wave transmission velocities values. The transmission velocity values determine the elastic deformational characteristics of the concrete, including the Young's, Bulk, and shear modulus values as well as Poisson's ratio and calculated strength values. These values are principally controlled by the presence of cracking, voiding or weak concrete. Appendix 1 has a more detailed description of the sonic/ultrasonic testing method.

Sonic/ultrasonic data was acquired with an automated system developed by NDT Corporation (pictured below). This system has eight (8) sensor mounted on axle so at every  $\frac{1}{2}$  rotation of the axle 4 sensors are in contact with the tie. Sensors are positioned so that there is a sensor near each end of each tie and a sensor inside of each rail. The system is equipped with two projectile energy source (one at end of the tie) that are activated when the sensor comes in contact with the

tie. There is a built in delay between the projectile energy sources so that a signal is produced at one end of the tie and at the other end. Unfortunately, one of the projectile sources was damaged during transit so this investigation was conducted with one energy source.



### **Discussion of Results:**

The results are listed as measured thickness resonant frequency values for Channels 1 and 4 (sensors at the end of the tie where delamination and cracking usually starts), shear/Raleigh wave velocity values recorded at sensors 2 and 3 inside the rail gauge and categorized in Table 1. The criteria used for rating the ties is based on a 1 to 5 scale used by many Railroads where:

- #1-No or minor defect- Thickness Resonant Frequencies of 7.5 to 8.5 KHz and shear wave velocities greater than 7,500 ft./sec
- #2-Minor cracking- Thickness Resonant Frequencies of 7.5 to 8.5 KHz and shear wave velocities less than 7,500 ft. /sec
- #3-Cracking isolated to within 4 to 5 inches of the tie end. Thickness Resonant Frequencies are higher than 8.5 KHz or lower than 7.5 KHz and shear wave velocities are in the range of 7,000 to 7,500 ft. /sec
- #4-End cracking is longer than 5 inches and interconnected and/or center cracking. Thickness Resonant Frequencies are higher than 8.5 KHz or lower than 7.5 KHz and shear wave velocities are in the range of 6,500 to 7,000 ft. /sec
- #5-Significant Cracking, Cracks are interconnected, Vertical Cracking near rail clips, Horizontal Cracking to or beyond rail clips. Thickness Resonant Frequencies are higher than 8.5 KHz or lower than 7.5 KHz and shear wave velocities are less than 6,500 ft. /sec.



The results indicate all but 4 of the ties are #1. Of the 4 that are not #1, 2 are #2 (minor cracking) and 2 have no results because sensors were not touching or were on a poorly coupled third rail plate.

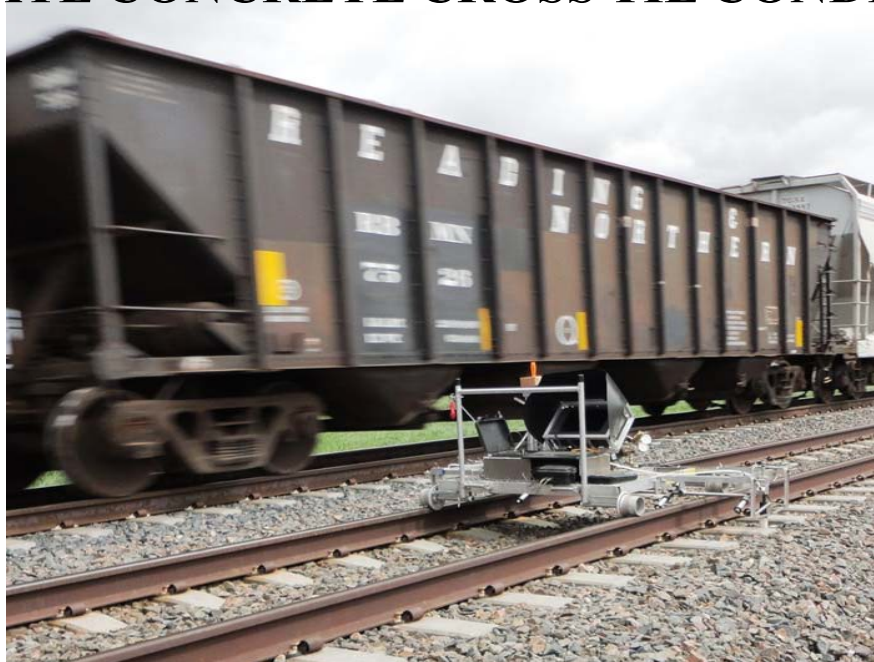
Table-1											
Tie #	Shot	West Tie end			East Tie end			Center	Rating	Comments	
		F 1	Vs 2		F 4	Vs 4		Cracking			
1	1	8.1	8.9		8.1	8.5		No	1		
2	2	8.2	8.4		8.1	8.7		No	1		
3	3	8.1	8.5		8.1	8.2		No	1		
4	4	7.7	8.8		8.2	7.9		No	1		
5	5	8.1	8.6		8.1	8.2		No	1		
6	6	8.1	8.4		8.3	7.7		No	1		
7	7	8.1	8.9		8.3	8.3		No	1		
8	8	8.1	9.0		8.1	7.6		No	1	Tamper damage	
9	9	7.9	8.8		8.0	8.2		No	1		
10	10	8.0	9.3		8.0	7.8		No	1		
11	11	8.5	9.3		8.0	8.6		No	1	Station 166+00	
12	12	7.9	9.2		8.0	7.8		No	1		
13	13	8.0	8.9		8.0	8.0		No	1	Plate east side	
14	14		9.1		7.5	7.0		No	2	Plate east side	
15	15	8.1	8.8		8.3	8.1		No	1	Tamper damage	
16	16	7.4	8.3		7.4	7.6		No	1		
17	17	8.1	9.5		7.7	8.4		No	1	Plate east Side	
18	18	8.2	8.5		7.5	8.3		No	1		
19	19	7.7	9.4		8.0	9.0		No	1		
20	20	8.5	9.3		8.0	8.5		No	1		
21	21	8.4	9.2		8.1	8.6		No	1		
22	22	8.3	8.5		8.3	8.2		No	1		
23	23	8.1	8.6		8.2	8.1		No	1	Plate east side	
24	24	8.2	8.5		8.4	8.3		No	1		
25	25	8.1	9.0		8.3	8.8		No	1		
26	26	8.2	8.7		7.6	8.8		No	1		
27	27	7.9	8.2		8.0	8.6		No	1		
28	28	7.7	9.3		7.9	8.2		No	1		
29	29	7.9	8.6		7.5	8.5		No	1		

Table-1												
30	30		8.0	8.9		8.0	8.2		No		1	
31	31			8.7		8.3	6.7		No		1	Plate east side
32	32		7.9	9.5		8.1	7.6		No		1	
33	33		8.0	8.2		8.4	7.7		No		1	
34	34		8.1	8.8		8.1	7.8		No		1	
35	Communication Box											
36	Communication Box Station 166+50											
37	35		8.1	9.1		8.2	6.8		No		2	
38	36		8.1	9.1		7.9	8.4		No		1	Plate east side
39	37		7.7	9.0		8.1	8.4		No		1	
40	38		7.7	9.1		7.5	8.2		No		1	
41	39		8.2	8.9		8.1	8.0		No		1	
42	40		7.5	9.3		7.6	7.3		No		1	
43	41		7.7	9.1		8.1	7.9		No		1	Plate east side
44	42		7.8	8.9		8.3	8.9		No		1	
45	43		7.5	9.1		7.6	8.7		No		1	
46	44		7.5	8.8		8.2	8.7		No		1	
47	45		8.0	9.0		sensor not touching						
48	46		8.5	8.8		sensor not touching						Plate east side
49	47		8.0	8.6		8.0	8.3		No		1	
50	48		7.5	8.9			7.6		No		1	
51	49		8.0	9.0		8.1	7.6		No		1	
52	50		7.5	8.9		8.1	8.0		No		1	
53	51		7.8	9.1		7.9	7.8		No		1	Plate east side
54	52		8.2	9.4		8.1	8.4		No		1	
55	53		8.1	9.0		7.5	8.6		No		1	
56	54		8.7	9.0		8.1	8.3		No		1	
57	55		8.0	9.0		7.4	8.3		No		1	
58	56		8.2	8.3		7.4	7.5		No		1	Plate east side
59	57		8.1	9.0		8.2	7.7		No		1	
60	58		8.2	8.7		8.0	8.1		No		1	

Table-1												
61	59		8.2	8.9		7.6	8.0		No		1	Sta. 167+00
62	60		7.7	9.4		sensor not touching					1	

**RESEARCH AND DEMONSTRATION  
PROJECTS SUPPORTING THE  
DEVELOPMENT OF HIGH SPEED AND  
INTERCITY PASSENGER SERVICE BAA-  
2010-1**

**July 2013 - PROGRESS REPORT  
ASSESSMENT OF PULSE VELOCITY TESTING  
TO RATE CONCRETE CROSS TIE CONDI**







153 Clinton Road • Sterling, MA 01564

Tel: 978-563-1327

Fax: 978-563-1340

July 2, 2013

Mr. Hugh B. Thompson II  
General Engineering-Track Research Division  
Office of Research and Development  
West Building- Mail Stop 20  
1200 New Jersey Avenue, SE  
Washington, DC 20590

Subject: Research Results Pulse Velocity Rating of Concrete Cross Ties  
Contract Number - DTFR53-12-C-00022, Requisition Number- 31120100024

Dear Mr. Thompson:

An evaluation of the use of nondestructive pulse velocity (PV) and echo (IE) testing to rate in service concrete cross ties was conducted along a section of the Union Pacific's line between Central City and Clark Nebraska on May 20, 21 and 22, 2013. This study was funded by FRA's "Research and Demonstration Projects Supporting the Development of High Speed and Intercity Passenger Service BAA-2010-1". Ninety one (91) ties were tested using sonic/ultrasonic impact velocity and echo measurements at four locations along a section of rail that was out of service for tie replacement.

The objectives of this testing was to determine:

- 1.) If sonic/ultrasonic impact velocity and echo data are affected by ballast and attached rails;
- 2.) Does ballast condition affect results?
- 3.) Can data be obtained in a production manner with an automated crosstie Testing system?

We would like to acknowledge the support provided to us by the Union Pacific Rail Road and in particular Mr. Dale Mellor, Mr. Stephen Ashmore, Mr. Eric Gehringer and Mr. Chris Roop.

This report presents the findings of this research project for your review and comment.

Sincerely,  
NDT Corporation

Paul S. Fisk

## TABLE OF CONTENTS

EXECUTIVE SUMMARY	Page 1
INTRODUCTION AND OBJECTIVES	Page 2
IMPACT VELOCITY AND ECHO MEASUREMENTS	Page 2
DISCUSSION OF RESULTS	Page 4
FIGURE 1	
TABLES	

## **1.1 Executive Summary:**

Nondestructive impact velocity and echo data were acquired with a handheld sensor array used in previous yard testing and with a rail mounted Automated Crosstie Testing (ACT) system to determine if ballast and attached rails would affect the data. A comparison of results indicates both systems have essentially the same results.

Impact velocity and echo data were acquired with the ACT system in a stretch of 50 crossties where numerous ties had been identified by railroad inspectors because of cracking to be replaced. Tie conditions were documented with photos for comparison with testing results. The comparison is subjective but does indicate ties that test at a 3 or 4 rating level have cracking or were identified (paint line) for replacement by railroad inspectors. These results indicate that impact velocity and echo data can be acquired on in service crossties in a production manner.

Impact velocity and echo data were also acquired on crossties that were in silt filled wet areas to determine if the changing ballast condition would affect results. Data acquired in these areas have reasonable velocity and thickness resonant frequency values and therefore it has been concluded that these ballast conditions do not adversely affect impact velocity and echo data.

Several ties with center cracking were tested. There was no significant drop in end to end wave velocity values. Close examination of some of these ties determined the center cracking although extensive does not extend the full thickness of the tie. Cracking did not propagate into prestressed region of the tie and therefor it is unlikely impact velocity data with the sensor spacing used for this testing will detect this cracking.

## **Introduction and Objectives:**

An evaluation of the use of nondestructive pulse velocity (PV) and echo (IE) testing to rate in service concrete cross ties was conducted along a section of the Union Pacific's line between Central City and Clark Nebraska on May 20, 21 and 22, 2013. This study was funded by FRA's "Research and Demonstration Projects Supporting the Development of High Speed and Intercity Passenger Service BAA-2010-1". Ninety one (91) ties were tested using sonic/ultrasonic impact

velocity and echo measurements at four locations along a section of rail that was out of service for tie replacement.

The objectives of this testing was to determine:

1. If sonic/ultrasonic impact velocity and echo data are affected by ballast and attached rails;
2. Do ballast condition affect results;
3. Can data be obtained in a production manner with an automated crosstie Testing (ACT) system?

Previous testing reported to the FRA in December 2012 has demonstrated that impact velocity and echo data can assess and qualify internal cracking and deterioration of concrete cross ties. This testing was conducted in Union Pacific and Amtrak Tie disposal areas where the ties were not in ballast and not attached to rails. This testing was to determine what affect if any ballast and attached rails have on impact velocity and echo data. This testing also evaluated the affects that different ballast conditions (wet silt filled ballast) might have on the Impact velocity and echo data.

Previous testing has been conducted with a handheld manual positioned array and energy source. For the Impact velocity and echo testing to be affective for commercial use, data will have to be acquired in a production automated fashion. NDT Corporation has a prototype Automated Crosstie Testing (ACT) system (See Photo on Page 4). To evaluate the data acquired by this system data were acquired on the same ties with both the handheld manual system and the ACT system.

Two other areas where ties were to be replaced were tested with the ACT system. After some of the ties had been removed, a visual inspection was conducted to map visible surface cracks and an assessment of how affected the testing was to rate ties.

### **Impact Velocity and echo measurements:**

Sonic/ultrasonic pulse velocity and impact data are acquired with an array of 4 sensors and a projectile impact energy source. Data acquired by sensors 1 and 2 closest to the impact source are used to access the condition and integrity of the tie from the end (impact location) to the inside of the rail seat (position of sensor 2). Pulse velocity data acquired at sensor 3 and 4 at the opposite end of the tie from the impact point, are used to evaluate for significant (into or through the prestressed core of the cross tie) vertical fractures at the center of the tie between rails. Each tie was impacted at each end and the sensor positions flipped so tie condition and integrity can be evaluated at both ends.

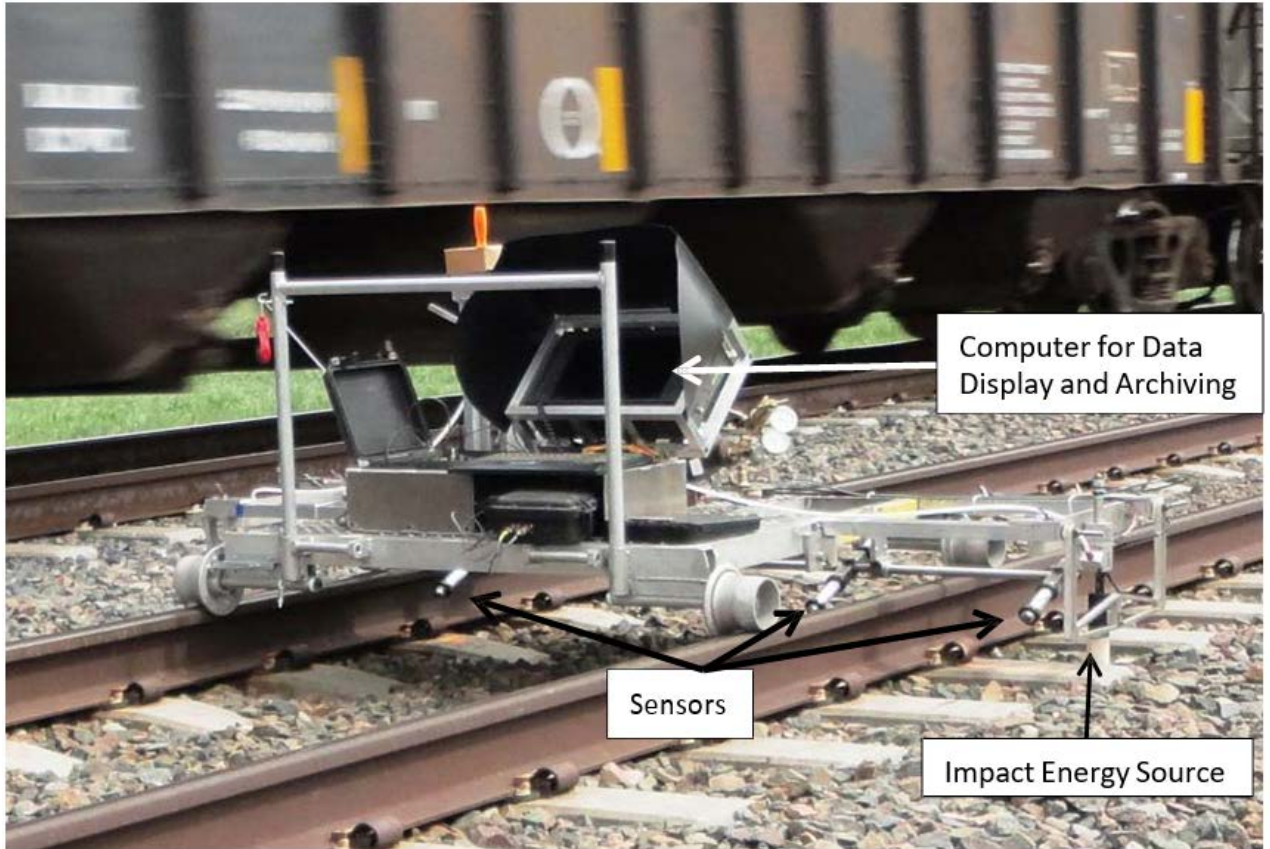
Data acquired by Sensor 1, closest to the impact energy source, is used to determine zero time for pulse velocity measurements and for impact echo data for the outside end of the tie. Data acquired by Sensor 2, on the inside of the rail seat, is used for pulse velocity measurements of the end of the tie and impact echo measurements in the rail seat area.

Impact echo measurements are affected by cracking in two ways: 1) micro cracking (not visible to the naked eye) and minor (short visible but not interconnected cracks) lower transmission velocities and lower measured resonant frequencies (Principal for ASTM 666); 2) delaminations or a series of interconnected horizontal cracks will result in no dominate resonant frequencies.

Pulse velocity measurements determine the time required for compressional and shear/Raleigh waves to travel a given distance. The velocity these waves (compressional, shear and Raleigh) propagate through the concrete is controlled by the elastic properties (Moduli values) and strength of the concrete which in turn is controlled by the amount/degree and severity of cracking. Typically unconfined 4,000 to 5,000 Psi concrete will have compressional wave velocity values in the range of 12,500 to 13,500 ft. /sec and shear wave velocity values in the range of 6,000 to 6,500 ft. /sec. In contrast, air has a compressional wave velocity of 800 ft. /sec and no shear wave (air has no shear strength). Compressional and shear waves are lower velocity in fractured concrete because the signals have to propagate through or around the cracks. The greater the density of cracks or the more severe the cracking, the lower the compressional and shear wave velocity values will be.

NDT Corporation's Automated Crosstie Testing (ACT) system (pictured on the next page) test both ends of the tie simultaneously. This system has a projectile impact system at each end of the tie. When the four sensors contact the top of the tie, energy impact at one end or the tie is activated and after 4 milliseconds the other end of the tie is impacted. Data is encoded for 8 millisecond so the first four milliseconds of data are for one end of the tie and the data from 4 to 8 milliseconds is used to evaluate the other end of the tie.





### Discussion of Results:

The results of the measurements made during this investigation are listed in Tables 1 for data acquired with the handheld and automated ACT system, Table 2 for a production run with the ACT system, and Table 3 in an area of silt filled wet ballast. Evaluation of results was done with field notes and photographs documenting crosstie conditions. Ties with paint stripes were identified by railroad inspectors for replacement. In many case the paint on the tie ends obscures cracking. Some ties were photographed after removal and these photographs are in the Tables.

Several ties with center cracking were tested. There was no significant drop in end to end wave velocity values. Close examination (see photo next page) of some of these ties determined the center cracking although extensive does not extend the full thickness of the tie. Cracking did not propagate into prestressed region of the tie and therefor it is unlikely impact velocity data with the sensor spacing used for this testing will detect this cracking.



### **Comparison of Manual system with ACT system:**

Data were acquired on 16 ties with the handheld sensor array used in previous testing and with the ACT system. The measured thickness resonant frequency values and shear wave velocities recorded on each end of these ties is listed in Table-1. Using the Tie Rating Decision Tree developed from data acquired and reported previously (Figure 1), a tie rating was determined for the handheld array data and the ACT data. The ACT results are within the reading error of the data of the handheld array results that is 10 of the 16 ties were rated exactly the same and the other 6 are within 1 rating of each other.

### **Does ballast condition affect results?**

At the Clark “Mud Fouled Area”, UP Tie numbers 529, 530, 531, 532 and 533 (Table 1) were tested with both the handheld and ACT systems. There was no noticeable difference in the data or rating for the ties that were in dry “good” ballast versus the ties that were in wet silt filled ballast. These ties have thickness resonant frequencies in or near the anticipated range of 7.5 to 8.5 KHz. Shear/Rayleigh wave velocity values are also in a range of 6500 to 8000 ft. /sec, a range detected in previous testing. ACT data were acquired in a second mud fouled ballast area, Table 3, ties NDT ID numbers 10 through 25 were identified by railroad inspectors for removal (see photos Table 3). These ties were rated 3, 4 and 5 by these results indicate the ballast, ballast conditions and attached rail do not affect the sonic/ultrasonic impact velocity and echo results.

## **Production Testing with the ACT System**

The ACT system was used at 2 locations (data in Tables 2 and 3) to obtain data in production manner. The objective of these test were to determine the quality of data and correlate results with visual conditions of the ties. The data quality check is to determine if there is noise from the system or the surroundings that are affecting data quality. The data quality is adequate for evaluating tie conditions but could be quieter. The recoil of the energy impact system is evident in the data. This can be rectified by isolating the energy system from the frame of the ACT system.

# Figures

## Decision Tree-Tie Rating UP Criteria

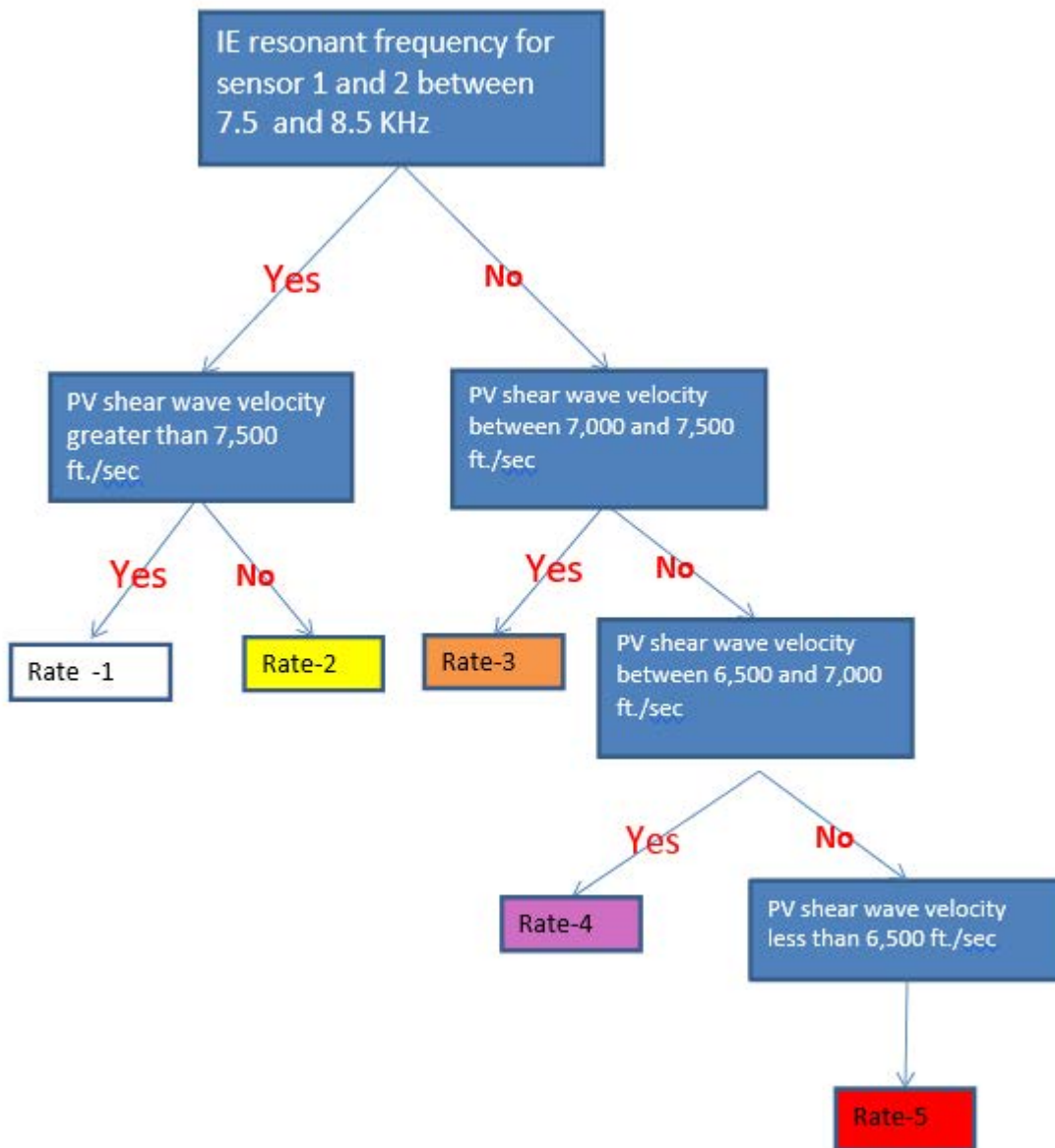


FIGURE 1



# Tables

TABLE-1 Clarks Mud Fouled Area





Tie	South Array Frequency	South Auto Frequency	North Array Frequency	North Auto Frequency	South Array Velocity	South Auto Velocity	North Array Velocity	North Auto Velocity	Array Ratings	ACT Ratings	South Side Photos	North Side Photos
520	7.38	7.45	7.67	7.42	7	7.93	7.28	7.20	Rank 3	Rank 3		
521	7.38	7.55	7.67	7.93	7.13	7.33	7.4	7.09	Rank 3	Rank 2		
522	7.52	7.58	7.67	7.83	7.5	7.57	7.5	7.38	Rank 1	Rank 2		
523	7.52	7.7	7.67	7.67	7.2	7.41	7.51	7.26	Rank 2	Rank 2		



TABLE-1 Clarks Mud Fouled Area

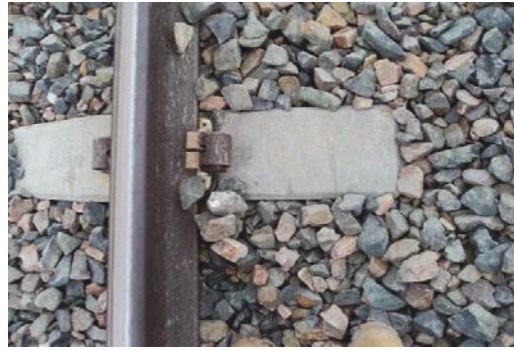


Tie	South Array Frequency	South Auto Frequency	North Array Frequency	North Auto Frequency	South Array Velocity	South Auto Velocity	North Array Velocity	North Auto Velocity	Array Ratings	ACT Ratings	South Side Photos	North Side Photos
524	7.52	7.59	7.74	7.6	7.29	7.41	7	7.29	Rank 2	Rank 2		
525	6.57	8.05	7.67	7.73	7.38	1.82	7	7.00	Rank 3	Rank 2		
526	7.6	7.71	7.6	7.73	7.38	8.03	7.66	7.23	Rank 2	Rank 2		
527	8.05	7.82	7.6	7.67	7.43	7.57	7.43	7.17	Rank 2	Rank 2		



TABLE-1 Clarks Mud Fouled Area





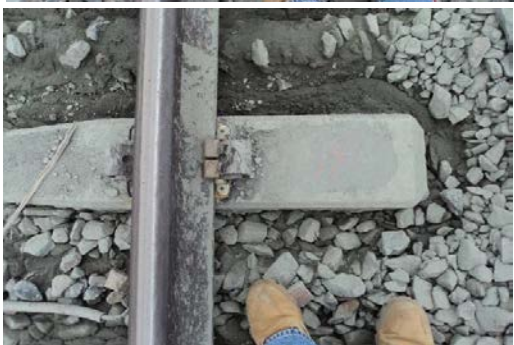



Tie	South Array Frequency	South Auto Frequency	North Array Frequency	North Auto Frequency	South Array Velocity	South Auto Velocity	North Array Velocity	North Auto Velocity	Array Ratings	ACT Ratings	South Side Photos	North Side Photos
528	7.6	8.39	7.82	7.82	7.36	7.33	7.11	7.50	Rank 2	Rank 2		
529	8.13	7.97	7.74	7.9	7.38	7.54	7.64	7.38	Rank 2	Rank 2		
530	8.05	8.13	7.82	7.82	7.22	7.59	7.22	7.17	Rank 2	Rank 2		
531	8.05	7.31	7.67	7.67	7.31	7.5	7.3	7.50	Rank 2	Rank 3		

TABLE-1 Clarks Mud Fouled Area

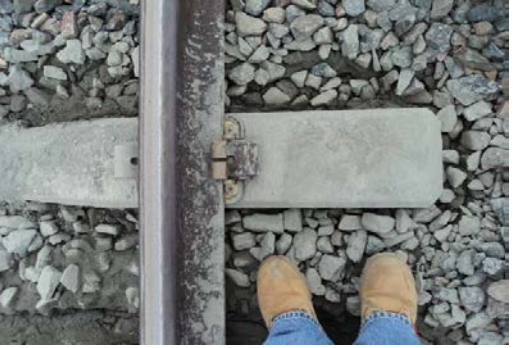





Tie	South Array Frequency	South Auto Frequency	North Array Frequency	North Auto Frequency	South Array Velocity	South Auto Velocity	North Array Velocity	North Auto Velocity	Array Ratings	ACT Ratings	South Side Photos	North Side Photos
532	8	8.21	7.82	7.82	7.55	7.54	7.26	7.29	Rank 2	Rank 2		
533	8.13	8.13	7.97	7.97	7.36	7.66	7.44	7.41	Rank 2	Rank 2		
534	7.5	7.52	7.82	7.74	7.16	7.66	7.17	7.79	Rank 2	Rank 1		
535	7.82	7.9	7.9	7.82	7.58	7.66	7.58	7.44	Rank 1	Rank 2		



Table-2 UP Ties 550 to 500 Ranking and Results With Photos




UP Tie #	NDT #	North End Frq	South End Frq	North S vel	South S vel	Rating	Photos	Photos	Photos	Photos	Photos
550	1	7.97	7.97	7.71	7.44	Rank 2					
549	2	7.82	7.82	7.49	7.76	Rank 2					
548	3	7.6	7.6	7.89	7.73	Rank 1					
547	4	7.03	7.03	7.63	1.21	Rank 5					
546	5	7.03	no data	7.59	no data	Rank 1					
545	6	7.6	7.6	7.84	7.56	Rank 1					
544	7	7.9	7.9	7.6	7.29	Rank 2					
543	8	7.52	7.52	7.33	7.32	Rank 2					
542	9	7.74	7.74	7.45	7.29	Rank 2					
P Tie #	10	7.67	7.67	7.31	7.44	Rank 2					
540	11	4	4	7.46	7.41	Rank 3					
539	12	8.05	8.05	7.96	7.69	Rank 1					
538	13	7.67	7.67	7.58	7.41	Rank 2					
537	14	7.67	7.67	7.49	7.26	Rank 2					
536	15	7.45	7.45	7.33	7.41	Rank 3					
535	16	7.74	7.74	7.33	7.41	Rank 2					

Table-2 UP Ties 550 to 500 Ranking and Results With Photos










UP Tie #	NDT #	North End Frq	South End Frq	North S vel	South S vel	Rating	Photos	Photos	Photos	Photos	Photos
534	17	7.24	7.24	7.11	6.90	Rank 4					
533	18	7.24	7.24	7.15	7.14	Rank 3					
532	19	7.24	7.24	7.25	7.29	Rank 3					
531	20	7.31	7.31	7.31	7.29	Rank 3					
530	21	7.45	7.45	6.94	7.00	Rank 4					
529	22	7.52	7.52	7.24	7.00	Rank 2					



Table-2 UP Ties 550 to 500 Ranking and Results With Photos

UP Tie #	NDT #	North End Frq	South End Frq	North S vel	South S vel	Rating	Photos	Photos	Photos	Photos	Photos
528	23	7.52	7.52	7.16	6.60	Rank 2					
527	24	7.38	7.38	7.23	6.64	Rank 4					
526	25	7.38	7.38	7.08	7.11	Rank 3					
525	26	1	1	7.27	7.00	Rank 3					
524	27	7.52	7.52	7.29	7.26	Rank 2					
523	28	1	1	7.39	7.00	Rank 3					
522	29	6.44	6.44	7.41	7.29	Rank 3					
521	30	7.45	7.45	7.17	6.77	Rank 4					
520	31	1	1	7.02	6.64	Rank 4					



Table-2 UP Ties 550 to 500 Ranking and Results With Photos















UP Tie #	NDT #	North End Frq	South End Frq	North S vel	South S vel	Rating	Photos	Photos	Photos	Photos	Photos
519	32	1	1	7.27	7.14	Rank 3					
518	33	7.67	7.4	7.1	6.90	Rank 4					
517	34	1	1	7.07	7.00	Rank 3					
516	35	7.45	7.45	6.89	7.56	Rank 4					
515	36	1	1	6.79	6.87	Rank 4					



Table-2 UP Ties 550 to 500 Ranking and Results With Photos







UP Tie #	NDT #	North End Frq	South End Frq	North S vel	South S vel	Rating	Photos	Photos	Photos	Photos	Photos
514	37	7.1	7.1	6.85	6.87	Rank 4					
513	38	6.57	6.57	6.61	6.77	Rank 4					
512	39	6.89	6.89	7	7.00	Rank 3					
511	40	7.17	7.17	7	7.00	Rank 3					
510	41	6.57	6.57	6.58	6.10	Rank 5					
509	42	6.63	6.63	6.85	6.87	Rank 4					
508	43	1	1	6.99	6.64	Rank 4					



Table-2 UP Ties 550 to 500 Ranking and Results With Photos

UP Tie #	NDT #	North End Frq	South End Frq	North S vel	South S vel	Rating	Photos	Photos	Photos	Photos	Photos
507	44	6.83	6.83	6.82	6.52	Rank 4					
506	45	6.83	6.83	6.68	6.55	Rank 4					
505	46	7.24	7.24	6.68	6.64	Rank 4					
504	47	6.83	6.83	7	7.00	Rank 3					
503	48	1	1	7.08	7.41	Rank 3					
502	49	6.83	6.83	6.88	7.86	Rank 4					

**Table-2 UP Ties 550 to 500 Ranking and Results With Photos**









UP Tie #	NDT #	North End Frq	South End Frq	North S vel	South S vel	Rating	Photos	Photos	Photos	Photos	Photos
501	50	6.38	6.38	7	7.26	Rank 3					
500	51	7.03	7.03	7.23	7.56	Rank 3					



Table -3 First Mud Fouled Area
















UP Tie #	NDT #	North End Frq	South End Frq	North S vel	South S vel	Ranking	Photos	Photos	Photos	Photos
111	1	7.89	8.05	7.58	7.79	Rank 1				
110	2	7.89	7.9	7.81	7.41	Rank 2				
109	3	7.89	7.82	7.48	7.66	Rank 2				
108	4	7.89	8.45	7.62	7.53	Rank 1				
107	5	4.28	4.08	7.52	7.63	Rank 3				
106	6	4.12	7.74	7.65	7.35	Rank 3				
105	7	4.2	7.1	7.03	7.00	Rank 3				
104	8	7.6	6.83	7.21	7.26	Rank 3				
103	9	7.1	7.38	7.22	6.87	Rank 4				



Table -3 First Mud Fouled Area

UP Tie #	NDT #	North End Frq	South End Frq	North S vel	South S vel	Ranking	Photos	Photos	Photos	Photos
102	10	7.1	6.96	7.23	7.35	Rank 3				
101	11	6.57	6.25	7.58	7.44	Rank 3				
100	12	6.63	7.03	7.12	7.59	Rank 3				
99	13	7.52	7.45	7.39	1.46	Rank 5				
98	14	4.04	4.08	7.15	7.06	Rank 3				
97	15	4	4	7.72	6.69	Rank 4				
96	16	7.89	6.63	7.85	7.47	Rank 3				

Table -3 First Mud Fouled Area

UP Tie #	NDT #	North End Frq	South End Frq	North S vel	South S vel	Ranking	Photos	Photos	Photos	Photos
95	17	4.04	6.83	7.92	7.69	Rank 3				
94	18	7.89	6.89	7.78	7.69	Rank 3				
93	19	7.89	7.24	7.52	7.66	Rank 3				
92	20	7.89	7.03	7.9	7.76	Rank 3				
91	21	7.74	6.96	7.46	6.90	Rank 4				
90	22	4	4	7.75	7.73	Rank 3				
89	23	8.62	7.17	7.62	7.53	Rank 3				
88	24	4.28	6.89	7.68	6.77	Rank 4				
87	25	4.12	7.67	7.82	7.41	Rank 3				



## Appendix D: Repeatability Testing Data – October 2013

Table 1 - First Run 633									
		South			North				
station(ft)	shot	f ch4	Vs ch3	Rating	f ch1	Vs ch2	Rating		Overall rating
0	633	7.5	7.18	2	7.81	7.56	1		2
2	632	8.42	8.33	1	8.3	8.17	1		1
4	631	7.81	7.92	1	7.69	8.04	1		1
6	630	8.42	8.44	1	8.3	8.44	1		1
8	629	7.96	7.34	2	7.69	7.75	1		2
10	628	7.08	7.60	1	7.57	7.31	2		2
12	627	7.32	7.60	1	7.69	7.38	2		2
14	626	7.93	7.85	1	7.57	7.32	2		2
16	625	8.42	7.98	1	8.3	8.13	1		1
18	624	4.1	7.82	2	7.93	7.45	2		2
20	623	7.81	7.57	1	8.06	7.97	1		1
22	622	8.42	8.23	1	8.06	1	2		2
24	621	7.69	7.14	2	7.81	7.97	1		2
26	620	4.58	7.79	2	7.2	7.9	1		2
28	619	4.21	7.88	2	7.2	8.12	1		2
30	618	8.06	8.60	1	8.17	8.53	1		1
32	617	7.76	7.51	1	7.69	8.11	1		1
34	616	8.3	7.82	1	8.42	1	2		2
36	615	7.2	8.09	1	7.2	7.91	1		1
38	614	4.14	8.02	2	8.42	808.92	1		2
40	613	8.52	8.09	1	8.42	7.76	1		1
42	612	7.45	7.82	1	7.69	1	2		2
44	611	7.45	7.98	1	7.81	7.79	1		1
46	610	7.45	7.63	1	7.69	1	2		2
48	609	8.67	7.66	2	7.93	7.89	1		2
50	608	8.3	8.37	1	8.42	8.37	1		1
52	607	8.54	7.69	1	8.42	7.98	1		1
54	606	8.42	8.12	1	8.3	8.37	1		1
56	605	8.3	8.48	1	8.18	8.29	1		1
58	604	8.06	7.76	1	8.18	7.9	1		1
60	603	8.42	8.33	1	8.42	1	2		2
62	602	8.06	7.60	1	8.06	7.99	1		1
64	601	7.32	7.72	1	7.57	1	2		2
66	600	7.63	7.45	2	7.69	7.75	1		2
68	599	6.71	7.51	2	7.81	7.74	1		2
70	598	7.45	8.02	1	4	7.84	2		2
72	597	7.93	8.02	1	8.1	1	2		2
74	596	7.57	7.63	1	7.69	7.56	1		1
76	595	8.3	8.02	1	8.42	7.91	1		1
78	594	8.42	8.02	1	8.3	7.81	1		1

Table 2 - Second Run 633									
station(ft)	shot	South			North			over all	
		f ch4	Vs ch3	Rating	f ch1	Vs ch2	Rating	Rating	
0	1	7.57	7.84	1	7.84	7.17	2	2	
2	2	8.37	7.87	1	8.42	8.46	1	1	
4	3	6.78	8.11	2	7.71	7.87	1	2	
6	4	8.12	8.83	1	8.42	7.98	1	1	
8	5	7.94	8.51	1	7.66	8.33	1	1	
10	6	1	8.36	2	7.44	8.33	1	2	
12	7	7.75	8.25	1	7.62	7.30	2	2	
14	8	7.23	8.29	1	7.73	7.49	2	2	
16	9	8.32	8.04	1	8.51	8.54	1	1	
18	10	6.82	8.25	2	7.36	7.83	1	2	
20	11	7.8	7.97	1	7.94	7.69	1	1	
22	12	8.46	7.84	1	8.46	7.76	1	1	
24	13	7.8	8.18	1	7.71	7.30	2	2	
26	14	8.61	8.33	2	8.46	8.21	1	2	
28	15	8.61	7.91	2	7.8	7.49	2	2	
30	16	7.66	8.22	1	7.71	8.42	1	1	
32	17	8.46	8.49	1	8.46	8.25	1	1	
34	18	8.42	8.48	1	8.37	7.56	1	1	
36	19	7.44	8.52	1	7.75	8.54	1	1	
38	20	7.53	7.91	1	7.44	7.80	1	1	
40	21	7.71	7.97	1	7.57	8.33	1	1	
42	22	7.75	7.87	1	7.75	7.83	1	1	
44	23	8.46	8.75	1	8.42	8.13	1	1	
46	24	8.46	8.22	1	8.27	7.83	1	1	
48	25	8.27	1	2	8.42	8.29	1	2	
50	26	8.27	8.48	1	8.32	7.98	1	1	
52	27	7.84	8.15	1	8.37	8.13	1	1	
54	28	8.46	8.48	1	8.42	8.50	1	1	
56	29	7.94	8.04	1	8.17	8.13	1	1	
58	30	7.62	8.04	1	7.57	8.17	1	1	
60	31	1	8.04	2	7.71	8.17	1	2	
62	32	7.66	8.79	1	7.75	7.80	1	1	
64	33	7.57	8.59	1	6.94	8.37	2	2	
66	34	7.94	8.48	1	7.94	8.37	1	1	
68	35	1	8.01	2	7.8	8.37	1	2	
70	36	8.46	8.71	1	8.32	1.00	2	2	
72	37	8.32	7.93	1	8.37	7.73	1	1	
74	38	7.57	8.51	1	7.53	8.21	1	1	
76	39	8.03	8.33	1	7.62	8.50	1	1	
78	40	7.8	8.33	1	7.53	7.98	1	1	
80	41	8.42	8.79	1	8.37	7.69	1	1	
82	42	8.32	8.79	1	8.37	7.80	1	1	
84	43	7.75	7.87	1	8.12	9.04	1	1	
86	44	7.89	8.55	1	7.4	7.73	1	1	

## **Abbreviations and Acronyms**

---

ASTM	American Society for Testing and Materials
ACT	Automated Concrete Tie
ACTT	Automated Concrete Tie Tester
VP	Compressional Wave Velocity
ESI	Engineering Services, Inc.
FRA	Federal Railroad Administration
IE	Impact Echo
IV	Impact Velocity
PV	Pulse Velocity
VS	Surface / Raleigh Wave Velocity